SKB

TECHNICAL REPORT 95-14

Consequences of using crushed crystalline rock as ballast in KBS-3 tunnels instead of rounded quartz particles

Roland Pusch

Clay Technology AB

February 1995

SVENSK KÄRNBRÄNSLEHANTERING AB
SWEDISH NUCLEAR FUEL AND WASTE MANAGEMENT CO
P.O.BOX 5864 S-102 40 STOCKHOLM SWEDEN
PHONE +46 8 665 28 00 TELEX 13108 SKB
FAX +46 8 661 57 19

CONSEQUENCES OF USING CRUSHED CRYSTALLINE ROCK AS BALLAST IN KBS-3 TUNNELS INSTEAD OF ROUNDED QUARTZ PARTICLES

Roland Pusch

Clay Technology AB

February 1995

CONSEQUENCES OF USING CRUSHED CRYSTALLINE ROCK AS BALLAST IN KBS-3 TUNNELS INSTEAD OF ROUNDED QUARTZ PARTICLES

Roland Pusch

Clay Technology AB

February 15, 1995

Keywords: Backfill, Ballast, Bentonite, Compaction, Compressibility, Crushed rock, Expandability, Grain size, Illitization, Piping

ABSTRACT

Backfills in KBS-3 tunnels with crushed crystalline rock as ballast (RB) can be prepared with the same gradation as "ideally" composed backfills with glacial sand as ballast (SB). RB backfills need more compaction energy to obtain the same density as SB backfills, but the physical properties at any density are fairly similar and RB backfills may therefore well be used although they have to be more effectively compacted on site than SB backfills. Such compaction can, however, be achieved in different ways. The chemical stability of both types is similar.

SAMMANFATTNING

Tunnelåterfyllningen i KBS-3 tunnlar med krossat, kristallint berg som ballast (RB) kan framställas med samma gradering som "idealt" sammansatta fyllningar med glacial sand som ballast (SB). RB-fyllningar kräver effektivare packning för att få samma densitet som SB-fyllningar, men de fysikaliska egenskaperna vid olika densitet är likartade och RB-fyllningarna kan därför användas men de behöver packas effektivare än SB-fyllningar. Sådan packning kan dock åstadkommas på flera sätt. Den kemiska stabiliteten är ungefär lika för båda.

LEGEND AND ABBREVIATIONS

Bentonite	Smectite-containing clay soil. The term is used here without reference to the origin.
Density	Bulk density $\rho = \frac{m_s + m_w}{V}$ where m_s = mass of solid constituents m_w = mass of porewater V = total volume Bulk dry density $\rho_d = \frac{m_s}{V}$ Grain density $\rho_s = \frac{m_s}{V_s}$ where V_s = volume of solid constituents
Glacial ballast	Natural more or less rounded soil material coarser than 2 μm. The term is used here for any natural soil extracted from eskers and other glacial deposits as well as from beach areas, irrespective of the origin of the minerals.
Grains	Solid constituents consisting of one or several minerals. The term is reserved here for ballast material.
Grain size	D_α is the grain diameter for α percent passing at sieving. The figure is obtained directly from ordinary grain size diagrams. $C_u = \frac{D_{60}}{D_{10}}$ is a measure of the uniformity of the grain size.
Grain shape	Sphericity $S = \sqrt[3]{\frac{b \cdot c}{a^2}}$ is a measure of how closely the general grain shape approaches the sphere, a, b and c being the largest, intermediate and smallest diameter, respectively. S=1 refers to the sphere.

Roundness $R = \frac{\Sigma r/R}{N}$ is a measure of the sharpness of the edges of grains. r is the radius of the individual edges, R the inscribed circle in the plane of observation and N the number of edges.

Splintery $F = \frac{s}{t}$ is a measure of the anisometry of grains, s being the size of the square meshes and t the width of the gratings at sieving by using these two sieving methods.

Particles — Soil constituents consisting of only one mineral. This term is reserved here for clay minerals with a size smaller than or equal to 2 μm.

Proctor (compaction) — The standard procedure for laboratory compaction of non-saturated soil material.

Void ratio — $e = \frac{V_p}{V_s}$

where

V_p = pore volume

Water content (ratio) — $w = \frac{m_w}{m_s}$

TABLE OF CONTENTS

SUMMARY

The consequences of replacing sand material of quartz type as ballast by crushed rock in tunnel backfills have been investigated. A basic question has been whether such replacement alters the hydraulic conductivity and compressibility as well as expandability, and also if the physical and chemical stabilities are altered.

The key factor is the microstructural constitution of the bentonite/ballast mixtures, which is primarily controlled by the grain size distribution of the ballast. It is preferably of Fuller's type with a low D_5 value in order to get both high densities and low conductivities. A number of examples show that the gradation of suitably composed artificial mixtures of glacial material can in fact be obtained by crushing crystalline rock without any processing.

The compactability of backfills with "quartz sand", termed SB in the report, is higher than that of backfills with crushed rock as ballast (RB). This means that for a given compaction energy, the density will be lower for RB backfills. This means that the hydraulic conductivity and compressibility of this sort of backfills will be somewhat higher than of SB backfills and that their expandability will be somewhat lower. Furthermore, the physical stability of RB backfills in terms of piping and erosion resistance will be somewhat lower than that of SB backfills. The chemical stability, which is determined by the conversion of the smectite component in the bentonite to illite, is practically independent of whether the ballast is pure quartz or rock with K-bearing minerals because the temperature in the backfill will be too low to yield significant smectite→illite conversion in the short heating period.

In order to reach the same densities of SB and RB backfills, which turn out to give fairly similar physical properties, the latter backfills need more effective compaction or, alternatively, a higher bentonite content. It is estimated that if the bentonite content in RB backfills is not increased while the density is enhanced to what is achievable, these backfills will serve equally well as SB backfills with the densities implied by the basic KBS-3 concept.

1 INTRODUCTION

1.1 SCOPE OF STUDY

The study reported here concerns possible consequences of replacing sand material of quartz type as ballast component in the backfill of KBS3-tunnels by crushed rock of granitic type. Such replacement may lead to a change in physical properties of the backfill in a short as well as long-term perspective. The most important properties are the hydraulic conductivity, compressibility and expandability, which - for given bentonite contents - all depend on the grain size distribution, bulk density, and on the physical and chemical stability of the bentonite component. The study is focused on these four properties of backfills with glacial components as ballast, representing "quartz sand", and with crushed rock as ballast.

2 BASIC CONCEPT

2.1 GENERAL

According to the recent documentation on repository design [1, 2] the backfill in the KBS3-deposition tunnels is proposed to be sand/bentonite mixtures that are prepared on the ground surface and transported down to the repository level.

The basic concept implies that the lower part of the tunnels is filled with material consisting of a mixture of 10 weight percent bentonite powder with its natural water content (10-15%) and 90 weight percent ballast with its natural water content (1-4%). This part of the backfill is applied and compacted layerwise and is expected to have a bulk density of 1.8-2.2 g/cm^3 with its initial water content, which corresponds to a density of 2.1-2.3 g/cm^3 at complete water saturation and to a dry density of 1.75-2.15 g/cm^3 [3]. The upper part is intended to be filled with a mixture of 20% bentonite and 80% ballast, with water added to reach approximately the optimum water content, i.e. 10-15% [3]. Shotcreting has been suggested for applying the upper part and Stripa experiments have indicated that this method can yield a bulk density of 1.1-1.8 g/cm^3, which at complete saturation corresponds to about 1.6-2.0 g/cm^3 (dry density ρ_d=1.00-1.64 g/cm^3). Figure 1 shows the robot system used for blowing in the upper part of the tunnel backfill. Figure 2 is a generalized section of a deposition tunnel with a 1.6 m diameter hole for a canister with spent fuel according to the basic KBS-3 concept.

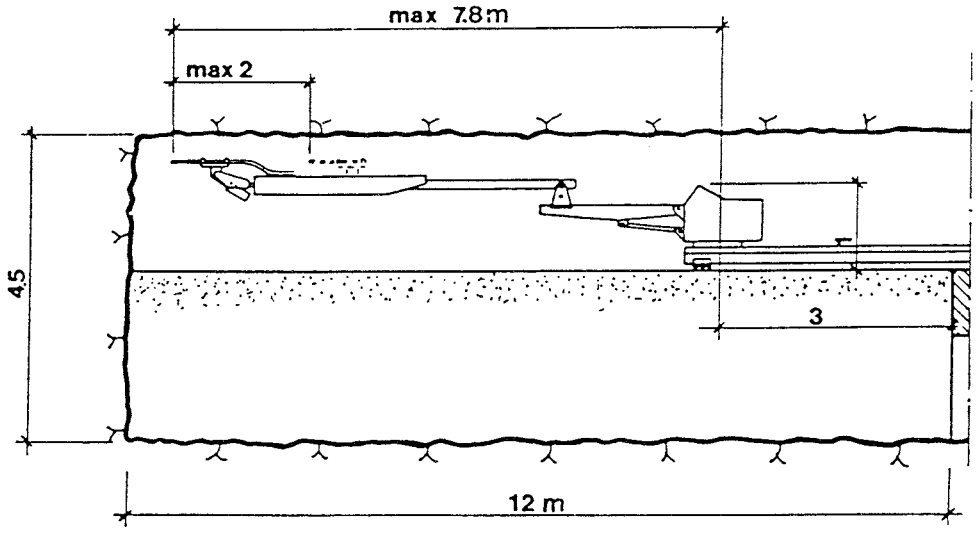

Figure 1. Shotcreting technique used for blowing in sand/bentonite in the Stripa BMT test [3]

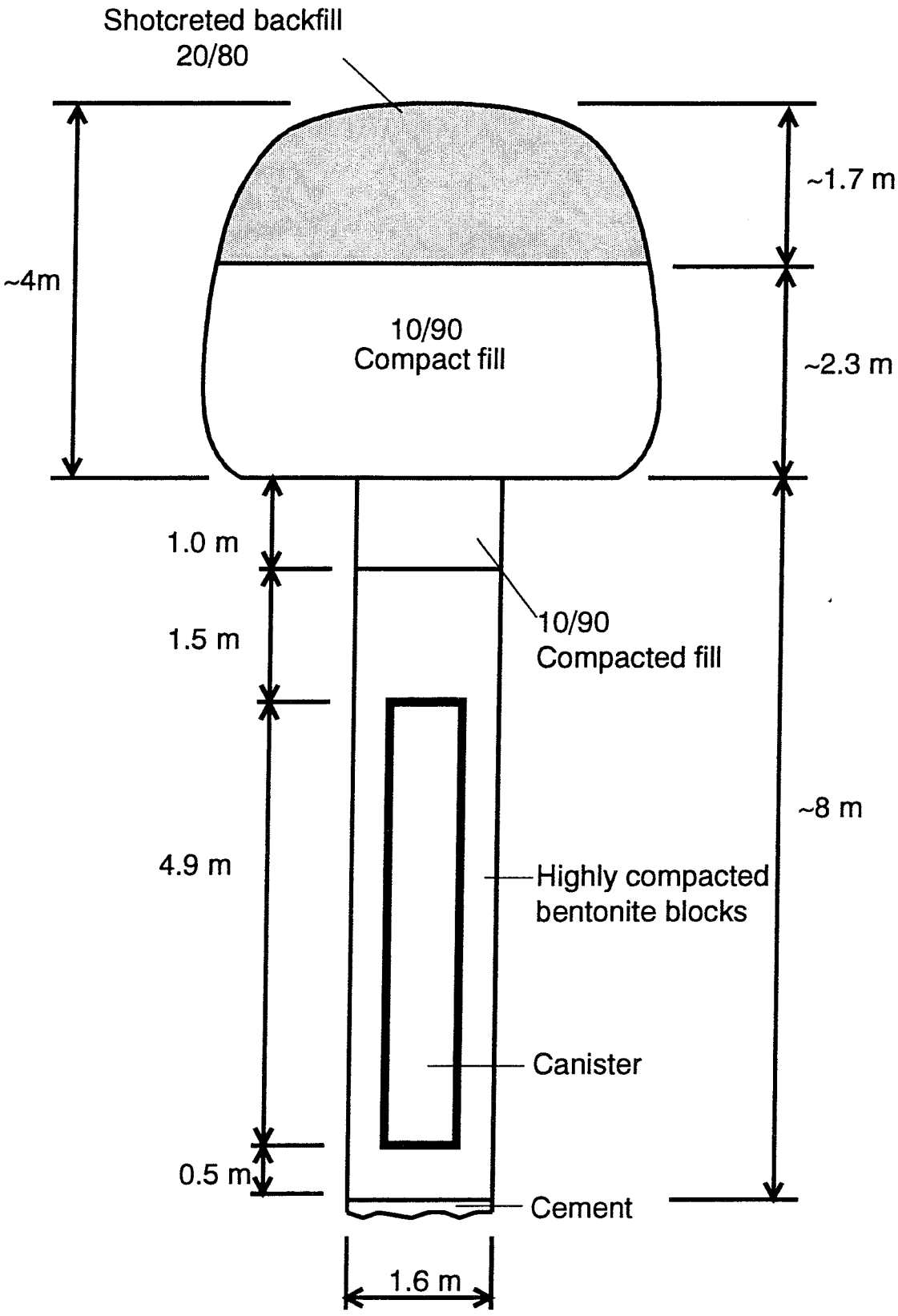

Figure 2. Schematic section of KBS3-tunnel according to the basic concept with application of the uppermost part of the backfill by use of shotcreting technique

3 CRITERIA

The backfill of KBS-3 deposition tunnels is primarily designed to perform in the following fashion [4]:

1. Reduce flow through the tunnel to become similar to or lower than that of the surrounding rock. A conductivity of about 10^{-9} m/s has been suggested as an upper value for the backfill.

2. Support the walls and roof of the tunnels so that rock fall and disintegration, yielding a significant increase in hydraulic conductivity of the nearfield rock, will be minimized.

3. Prevent unacceptable upward expansion of the highly compacted bentonite in the deposition holes.

The required supporting power and resistance to compression mean that the density of the bentonite in the ballast voids must be sufficiently high, implying a high bulk density of the mixture.The tightness criterion requires that piping and erosion do not alter the distribution of the bentonite component in the backfill in the application phase and afterwards, and also that chemically induced degradation of this component does not reduce its sealing power. It is therefore necessary to investigate how the backfill performs with respect to the influence of hydraulic gradients and chemical attack and we will consider both issues here. They both depend, more or less, on the microstructural constitution, which therefore deserves a short presentation as a basis of the report.

4 THE MICROSTRUCTURAL CONSTITUTION OF BACKFILLS

4.1 BALLAST MATERIAL

General principles

The distribution of grains of different size determines the size and connectivity of the voids of any soil and thereby its hydraulic conductivity and compactability. Theoretical as well as experimental investigations have shown that for non-clay materials with well-rounded grains, the best size distribution of spherical particles to yield minimum porosity is represented by Fuller's curve (Figure 3). As an example, very dense layering has been obtained by using correspondingly composed concrete ballast (a, b, c in this figure) for the preparation of the bottom bed of the Forsmark silo (ρ_d~2.15 g/cm^3).

Non-spherical grains and grains with a low degree of roundness, i.e. with rough surfaces, commonly give lower densities than spherical ones for a given grain size distribution and compaction effort except when the grains break down due to abrasion [5]. This is well illustrated by compression tests of four types of material with the grain size distributions shown in Figure 4. The compressometer was of ring-type with 0.5 m diameter and 1 m height [6]. The application of the materials, from which smaller grains than 4 mm had been removed, was made in the following three modes:

- Piece-by-piece application.
- Plunging.
- Plate vibration of 10 cm layers at a vibrator load of 16 kg.

The major data were as given in Table 1, from which one finds that the similarly sized grain assemblages of spherical and well rounded material (No. 4) and blasted rock (No. 7) had quite different densities in uncompacted form; e_{max}=0.70 and e_{max}=0.93, respectively, while they were equally dense after effective compaction, i.e. e_{min}=0.50. The high e-value of the blasted, angular material (No. 6) is explained by the open network formed by the anisometric grains, which were broken and formed finer fragments under heavy compaction, yielding almost the same density as for the spherical, well rounded grains of the glacial material. The splintery factor is defined as f=b/c, Figure 5. In road and earth dam construction, suitable crushed rock material commonly has $1.2<f<1.35$.

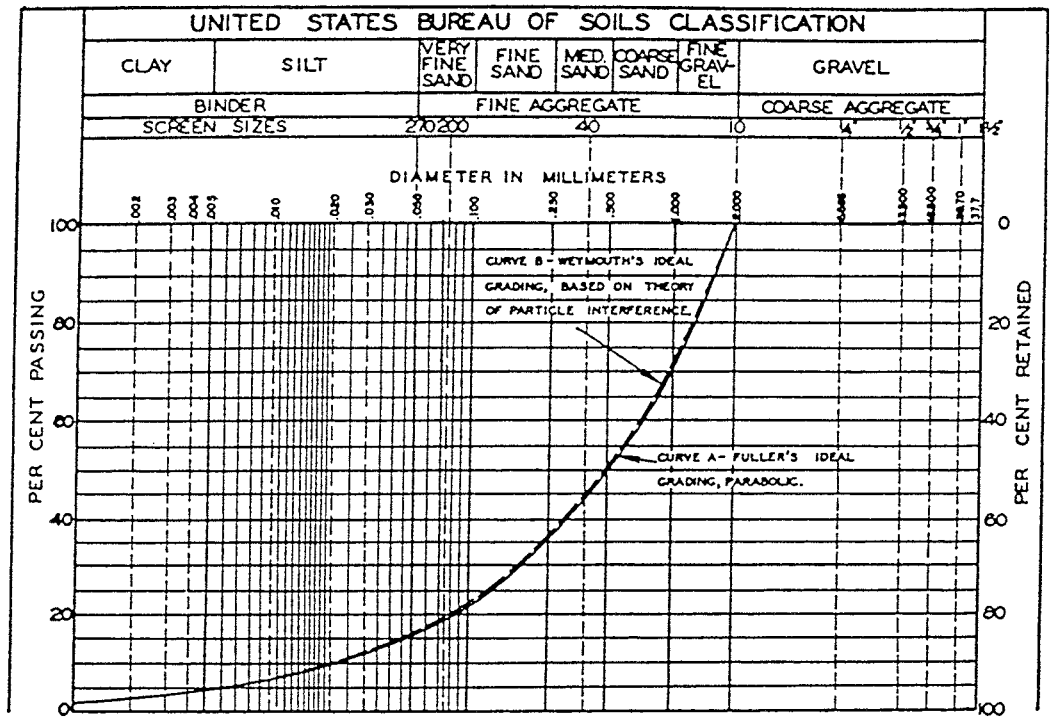

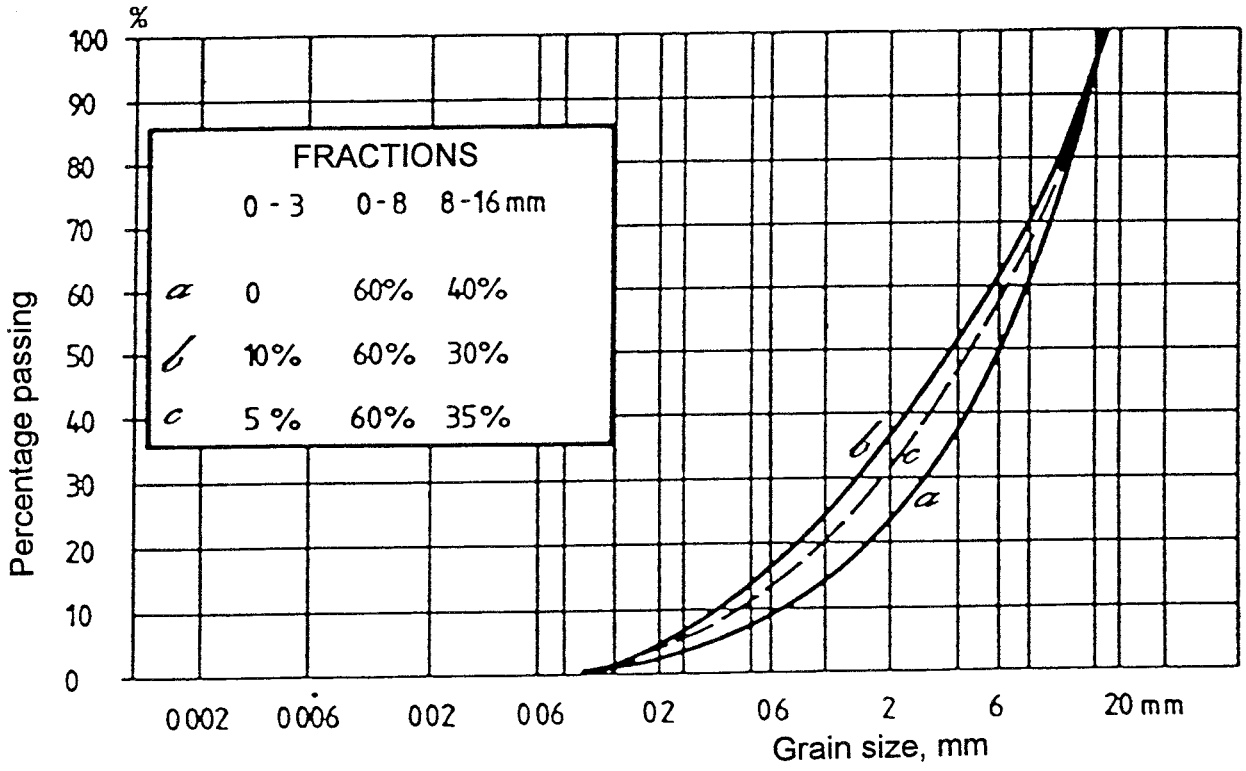

Figure 3. *Suitable ballast grain distributions for yielding high densities. Upper: Fuller's curve. Lower: Forsmark concrete ballast used for preparing the low-permeable bottom bed on which the silo rests. a, b and c were tested with respect to the compaction properties and "b" was finally selected.*

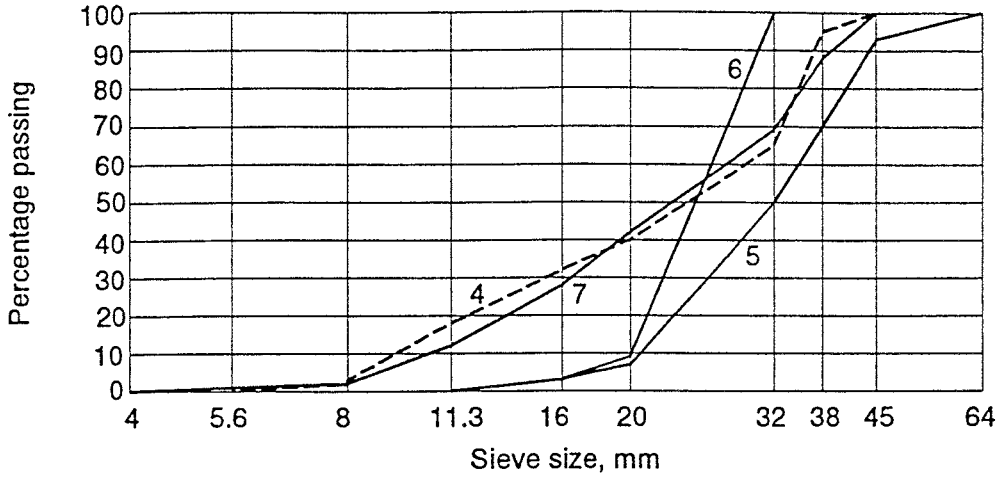

Figure 4. *Size distribution (b-diameter) of four coarse materials. 4 is a mixture of well-rounded glacial material, 5 is crushed fine-grained granite, 6 is crushed quartzite and 7 blasted gneiss rock [6].*

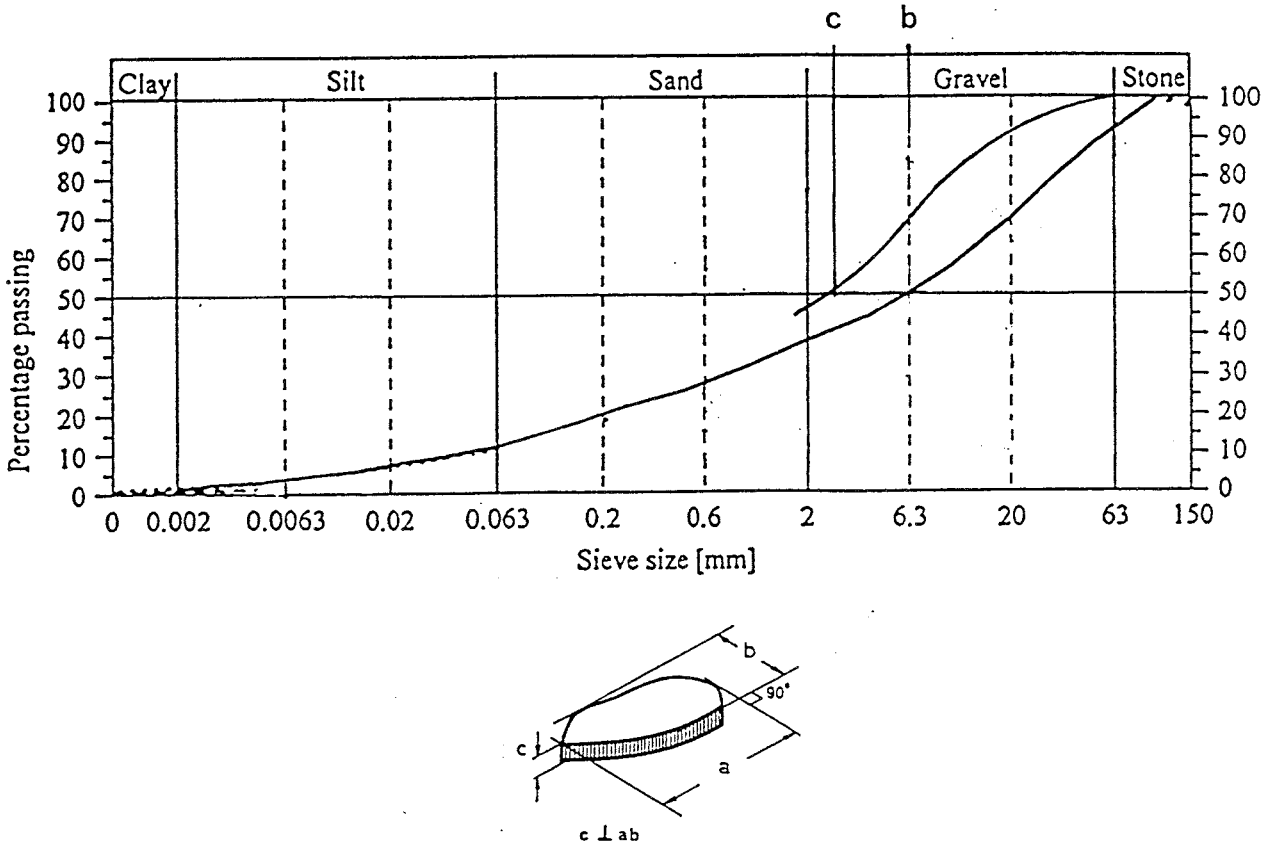

Figure 5. *Evaluation of the splintery factor from sieving using ordinary square mesh sieves yielding b-dimensions and rod sieves yielding c-measures*

Table 1. Granulometric data of coarse rock material.

Material	D_{50} mm	$C_u=D_{60}/D_{10}$	Splintery factor, f	Sphericity	Roundness	e_{max}	e_{min}	ρ_s, g/cm^3
Glacial (4)	25	3.1	1	0.71	0.38	0.70	0.50	2.69
Crushed granite (5)	32	1.65	1.17	0.69	0.10	0.94	0.59	2.68
Crushed quartzite (6)	25	1.30	1.33	0.64	0.22	0.97	0.53	2.64
Blasted gneiss (7)	23	2.6	1.32	0.63	0.18	0.93	0.50	2.69

In the coarse fraction of certain types of crushed crystalline rock, the shape of small and large grains may be elongated (or bladed) but not of those of intermediate size (Figure 6). This can explain the rather high splintery factor of the quartzite but the fact that the e_{min}-value was still low may be due to breakage of "fibrous" particles in the compaction phase. It is estimated that the rather high e_{min}-value of the crushed granite was due to very high strength and resistance to compression due to very sharp corners and irregular surface topography, manifested by the low roundness (0.10).

Finnish investigations of crushed Hästholmen rapakivi granite with the granulometry shown in Figure 7 gave a dry density of 2.01 g/cm^3 (Proctor) (w=4%) and a hydraulic conductivity of 10^{-5} m/s [7]. Addition of ground rock to the various size distributions shown in this figure gave conductivities down to 10^{-7} m/s.

The IVO-5 material with 29% ground rock and 71% crushed rock was selected for preparation of bentonite/ballast mixtures.

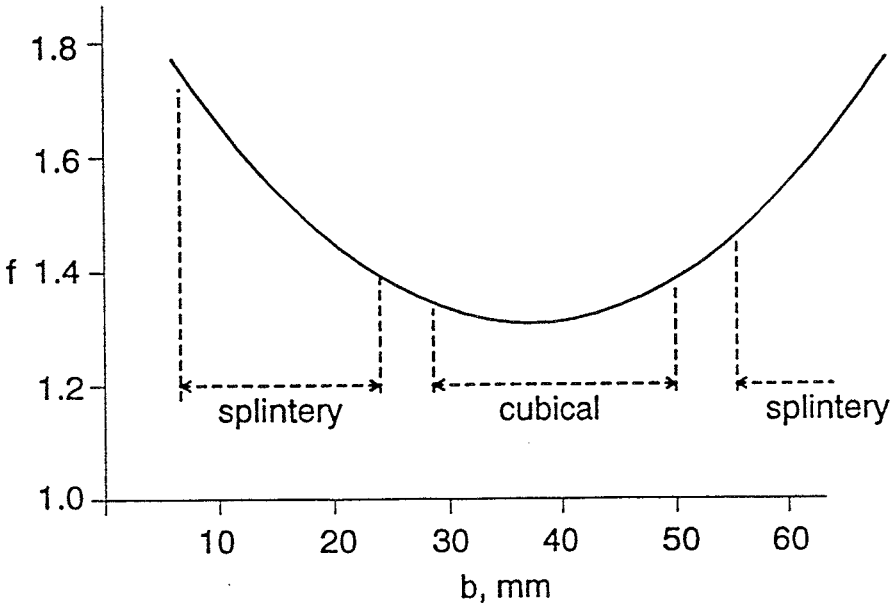

Figure 6. Empirical relationship between size and shape of crushed rock material (After von Matern)

In contrast to the crushed Stockholm Granite (No. 5 in Figure 4), from which material finer than 4 mm had been removed, Finnish crushed rock (IVO-1 in Figure 7) contained material as fine as 2 μm. This is always the case for effectively crushed rock but the content of fines may vary. Figure 8 shows that the general shape of the grain size distribution curve may be similar of crushed rock (Morgårdshammar) and blasted rock (Boliden). The crushed material has almost the same gradation as the Finnish material (IVO-1 in Figure 7), which is explained by their similar structure and mineralogy. A third example of similar type is crushed rock from Romeleåsen, Skåne (Figure 9). However, depending on the natural rock structure the gradation may be different and yield more fine material. This is particularly obvious for feldspar-rich rock as illustrated by the diagram in Figure 10, which shows the grain size distribution of crushed rock from the nuclear plant area at Simpevarp (Oskarshamn) [8].

Importance of the fine tail of the gradation curve

Naturally, very fine material in dense layering gives narrow, tortuous passages for flowing water and hence a low hydraulic conductivity irrespective of the gradation. This suggests that the fine tail of the grain distribution curve is important, which has also been demonstrated by several investigations [9].

Starting from Darcy's basic flow equation one can express the unit flux q as a function of seven characteristic parameters:

$$q = f(i, \gamma, \mu, D_x, S, \eta, n) \qquad (1)$$

where

i = hydraulic gradient
γ = density of fluid
μ = viscosity of fluid
D_x = representative grain size
S = gradation factor expressing the shape of the grain distribution curve
η = grain shape factor
n = porosity

By means of dimensional analysis the following expression can be derived [9]:

$$q = i(\gamma/\mu)k_0 \qquad (2)$$

and

$$K = (\gamma/\mu)k_0 \qquad (3)$$

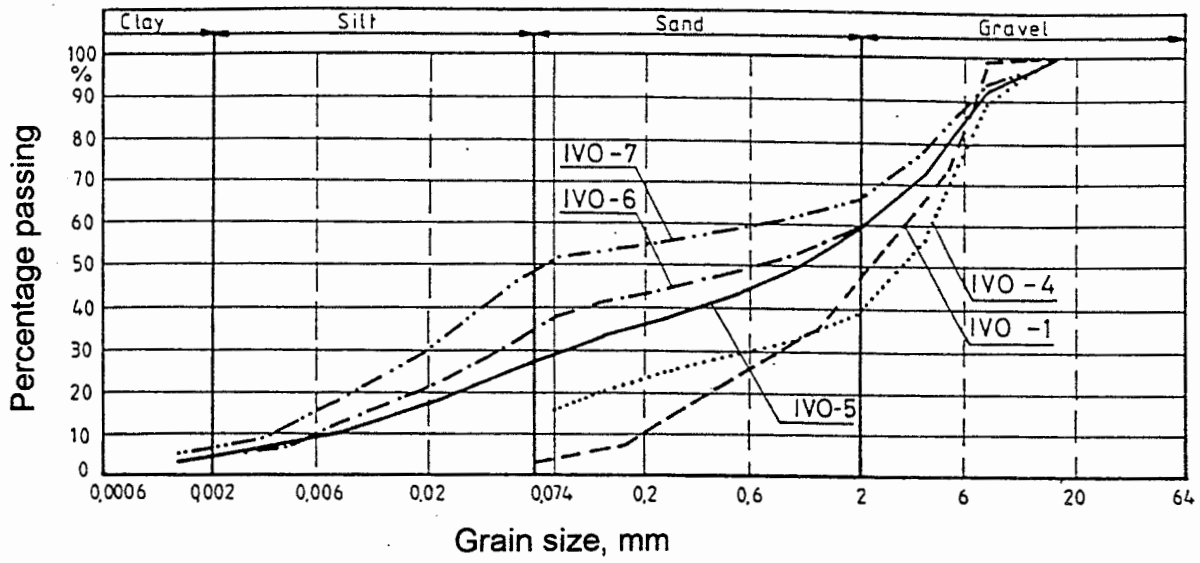

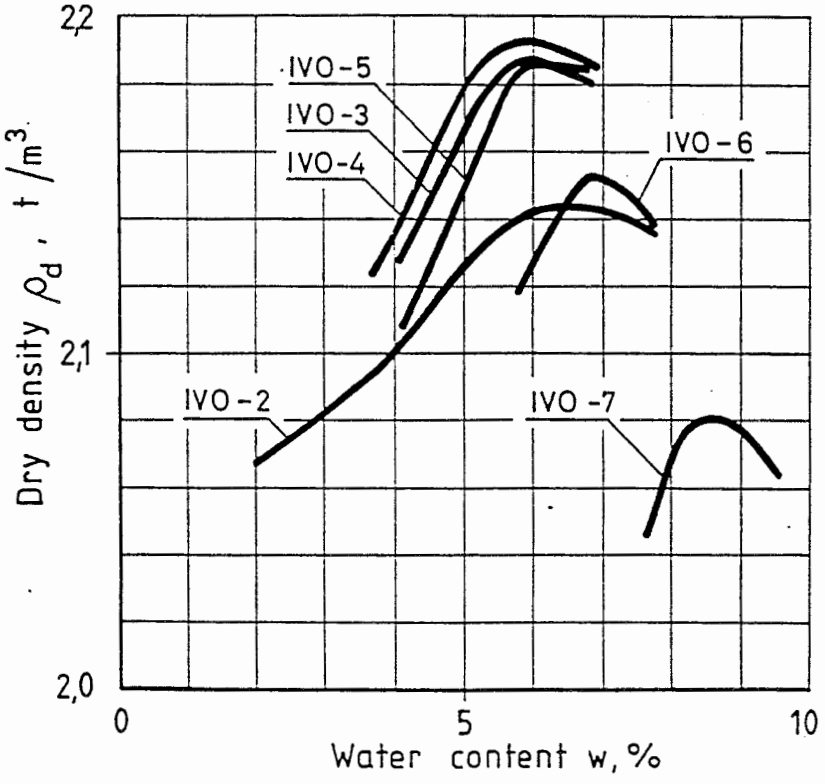

Figure 7. *Compaction curves of mixtures of crushed rock and ground rock according to Finnish studies [7]. IVO-1 in the upper diagram represents the crushed rock with no admixture of ground rock.*

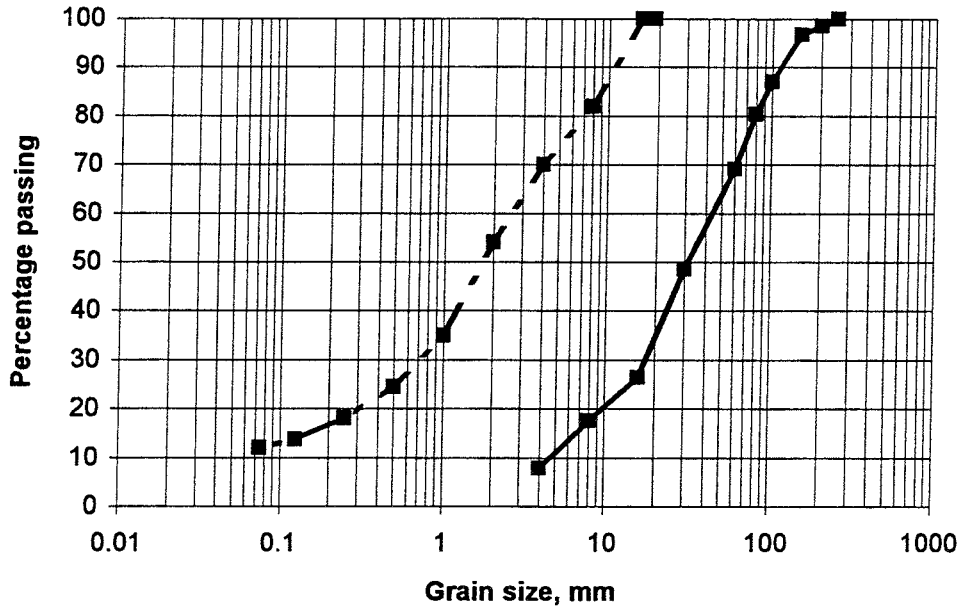

Figure 8. *Grain size distribution of blasted crystalline rock of granitic type (right curve, Boliden) and crushed rock (left curve, Morgårdshammar)*

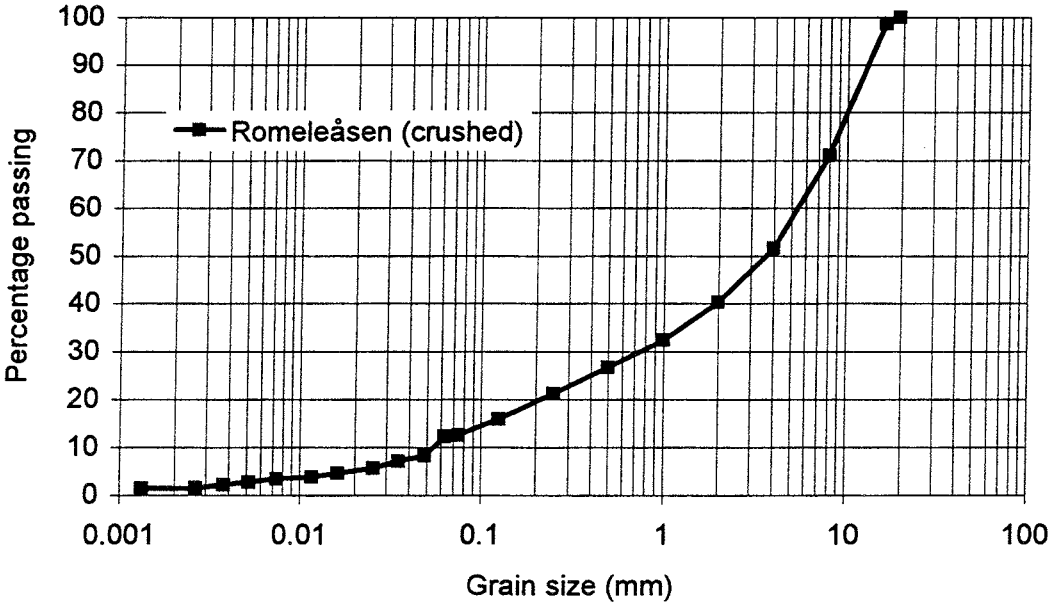

Figure 9. *Grain size distribution of crushed granitic rock from Romeleåsen*

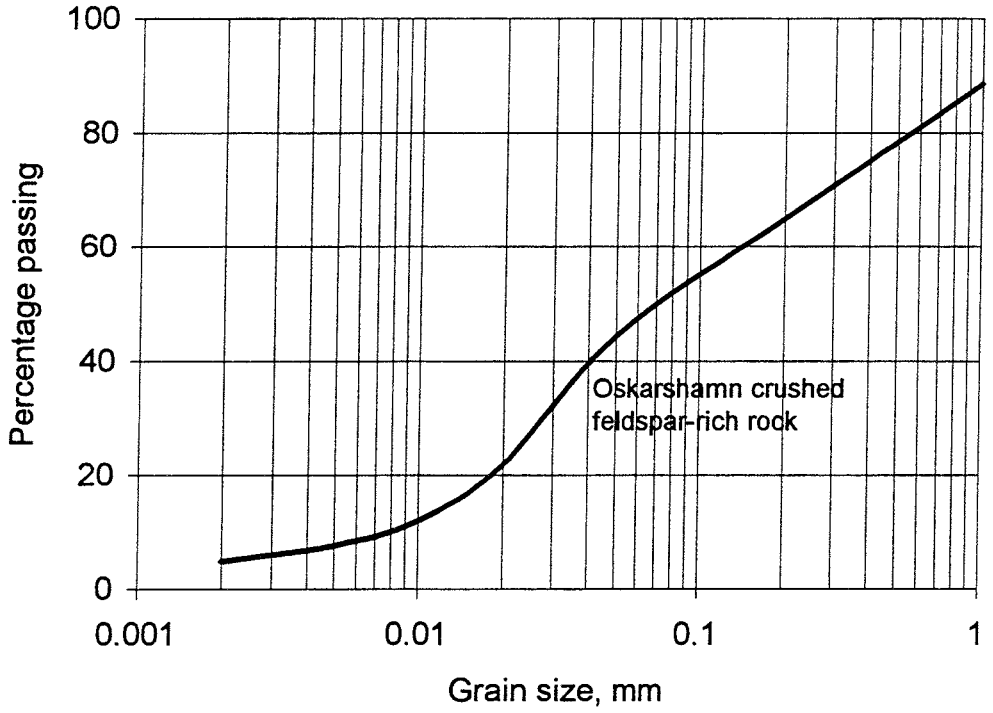

Figure 10. *Grain size distribution of crushed rock from the construction site of the nuclear plant at Simpevarp [8]*

where

K = experimentally determined hydraulic conductivity
k_0 = "specific permeability" of dimension (length)^2 describing the geometry and size of the void network

k_0 can be expressed as

$$k_0 = \beta_\alpha \cdot D_\alpha^2 \qquad (4)$$

where

β_α = dimensionless factor describing the geometry (but not the size) of the void network
D_α^2 = measure of the cross-sectional area of the average pore channel

Eq. (3) gave the plottings in Figure 11 of *log* k_0 and *log* K versus *log* D_5, which is the percentage of particles representing the 5th percentile of the grain size curve. The diagram shows that the plottings form bands for C_u=1-3 and C_u >3n ($C_u = D_{60}/D_{10}$), the first one representing relative uniform grain size and the other flatter grain size curves.

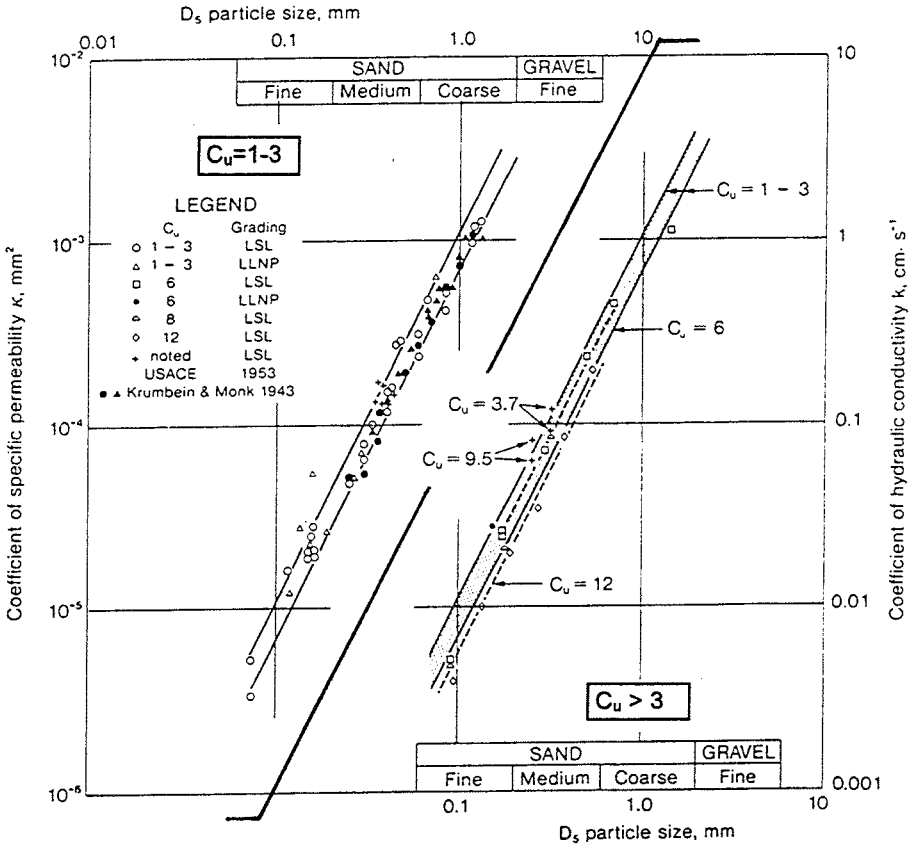

Figure 11. *Specific permeability in mm^2 versus D_5 grain size in mm.*

One finds from Figure 11 that C_u is not a determinant of the hydraulic conductivity but that D_5 is the key parameter. Choosing different values for α in D_α the bands in Figure 11 will change their relative positions but it has been concluded that $\alpha = 5$, i.e. D_5, is the conductivity-controlling grain size independently of the size distribution of the rest of the mineral assemblage, provided that the gradation curve is not discontinuous [9]. Taking for instance $D_5 = 0.1$ mm, for which the expected average conductivity is about 10^{-4} m/s, while for $D_5 \sim 0.3$ mm it is 10^{-3} m/s. Extrapolation suggests that the conductivity may be as low as 10^{-5} m/s for $D_5 \sim 0.05$ mm. This fits fairly well with the Finnish investigations referred to in the comments to Figure 7.

The importance of the tail of the distribution curve has been recognized in the composition of earth dam cores for many decades and it was also a major issue in the preparation of the backfill of the BMT drift at Stripa, for which the components specified in Table 2 were used. The coarser fractions, which were rich in quartz, were of glacial origin, while the "filler" consisted of crushed and finely ground feldspar-rich rock. Figure 12 shows the grain size distribution of the ballast. It is of Fuller-type with a tail that yields $D_5 = 0.008$ mm, which would suggest that the hydraulic conductivity of very well compacted material is in the range of 10^{-6} - 10^{-5} m/s. The Simpevarp material in Figure 10 is estimated to have the same or even lower conductivity if it is very effectively compacted.

Table 2. Backfill data of the BMT experiment

Na-bentonite* content in weight percent of total backfill	Ballast components	Average water content of mixed backfill	Mode of application
10%	≤ 0.3 mm "filler"; 20% of total ballast 0.1-1.0 mm sand; 50% of total ballast 0.5-2.0 mm sand; 30% of total ballast	10	Layer-wise application and compaction
20%	≤ 0.3 mm "filler"; 20% of total ballast 0.1-1.0 mm sand; 50% of total ballast 0.5-2.0 mm sand; 30% of total ballast Quartzite gravel added	15.5	Shotcreting technique

*The water content of the bentonite ranged between about 9 and 13%. The water content of the ballast was about 3%.

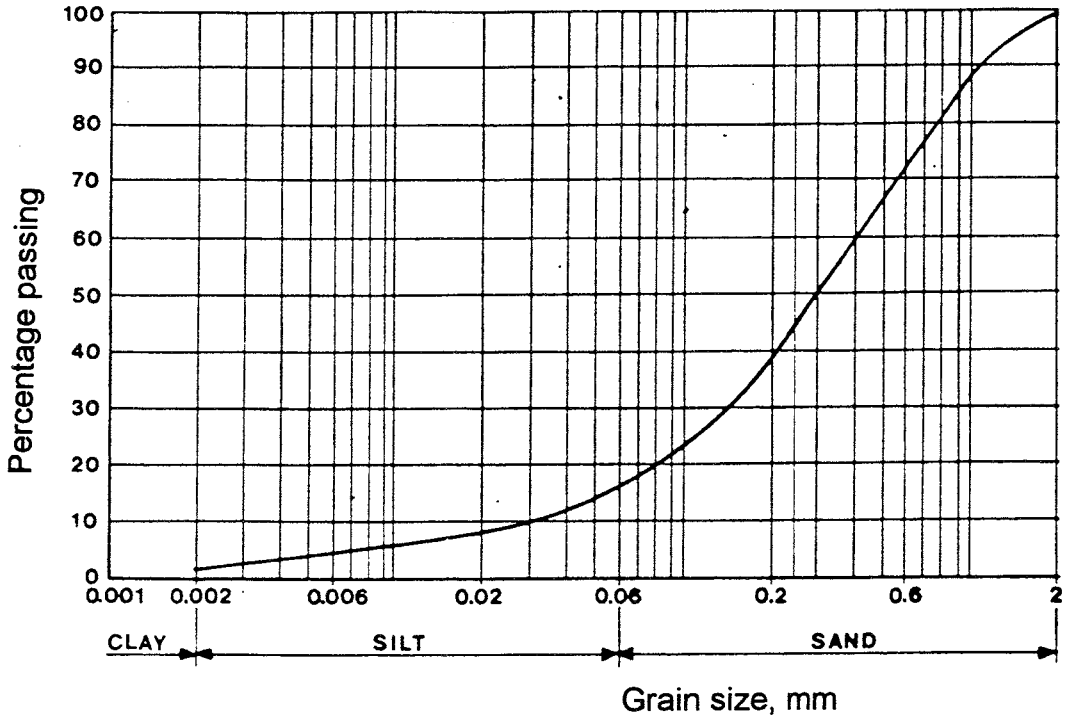

Figure 12. Experimentally determined grain size distribution of the artificially composed ballast used for the BMT experiment.

4.2 BENTONITIC BACKFILLS

General composition principles

The bentonite component of backfills of KBS-3 type must be in a sufficiently fine-grained form to fit into the voids between the ballast grains (Figure 13). This can be achieved by using very finely ground powder, which offers some practical difficulties like the release of dust in the mixing process and also the formation of a clay coating of the ballast grains when the finely dispersed smectite material comes into contact with the hydrated surface of the ballast grains. There is probably an optimum size distribution of the bentonite granules that is still not known.

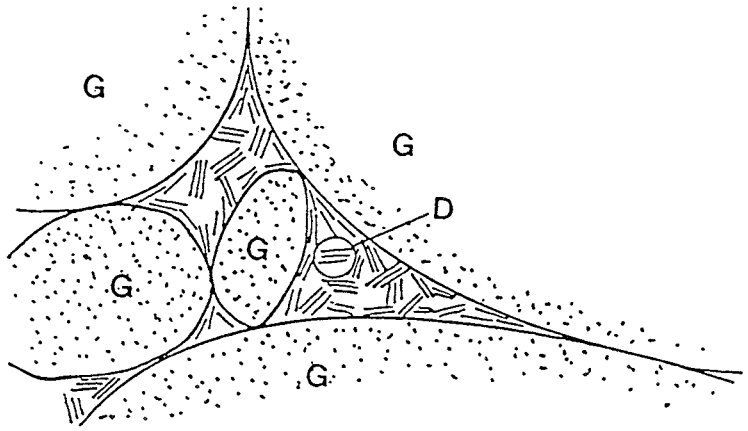

Figure 13. Schematic picture of the microstructure of bentonite-poor mixtures. G = ballast grains, D = clay component

4.2.1 Bentonite content and density

It is estimated from various studies that the bentonite content vs. dry density relation is of the type shown in Figure 14, which makes it possible to refer to the ballast void size distribution and to the degree of compaction. The relation in this figure concerns BMT ballast (Figure 12) and granulated MX-80 bentonite (Figure 15), the mixture being compacted to 100% Standard Proctor [10]. Using the General Microstructural Model (GMM) for the bentonite component [11], and taking the clay in the ballast voids to be uniformly distributed with a density that is controlled by the void size of the ballast material one obtains the diagrams in Figures 16 and 17. This sort of microstructural analysis can be made for any ballast material for estimating the required minimum clay content for 100% filling of the ballast voids.

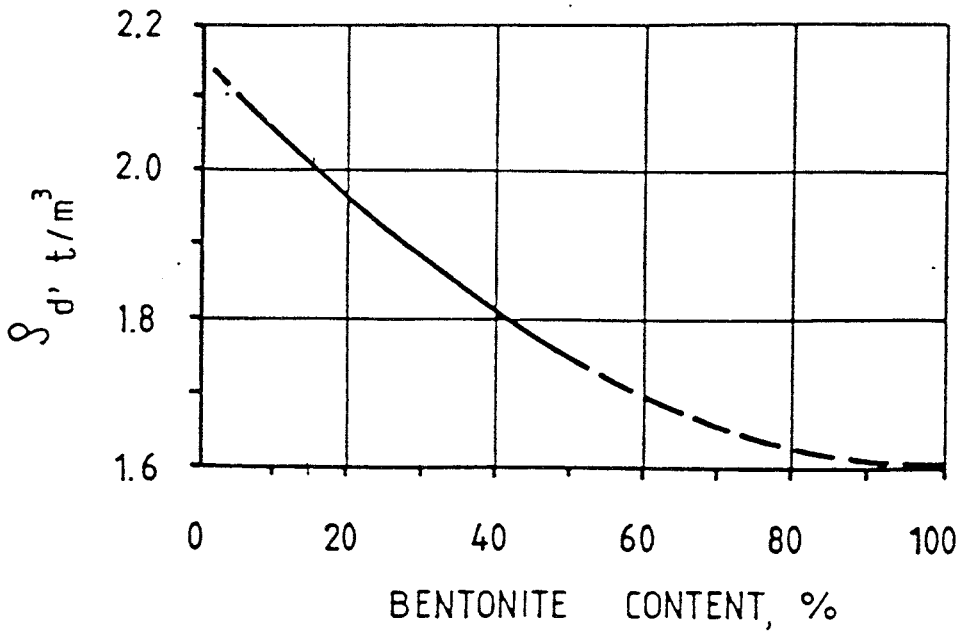

Figure 14. *Relationship between bentonite content and dry density. The relationship refers to mixtures of MX-80 bentonite and BMT ballast material at 100% Standard Proctor [11]*

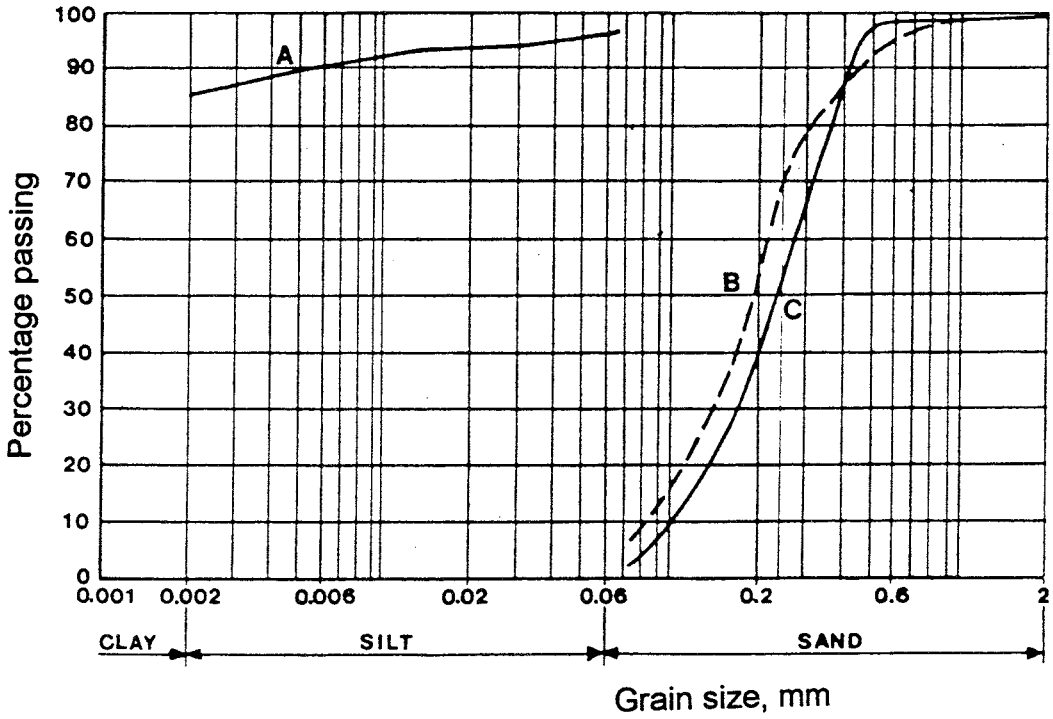

Figure 15. *Grain characteristics of the MX-80. A) represents the size distribution of dispersed material indicating a very high frequency of clay particles. B) and C) represent curves representative of the aggregated powder sieved in an air-dry condition.*

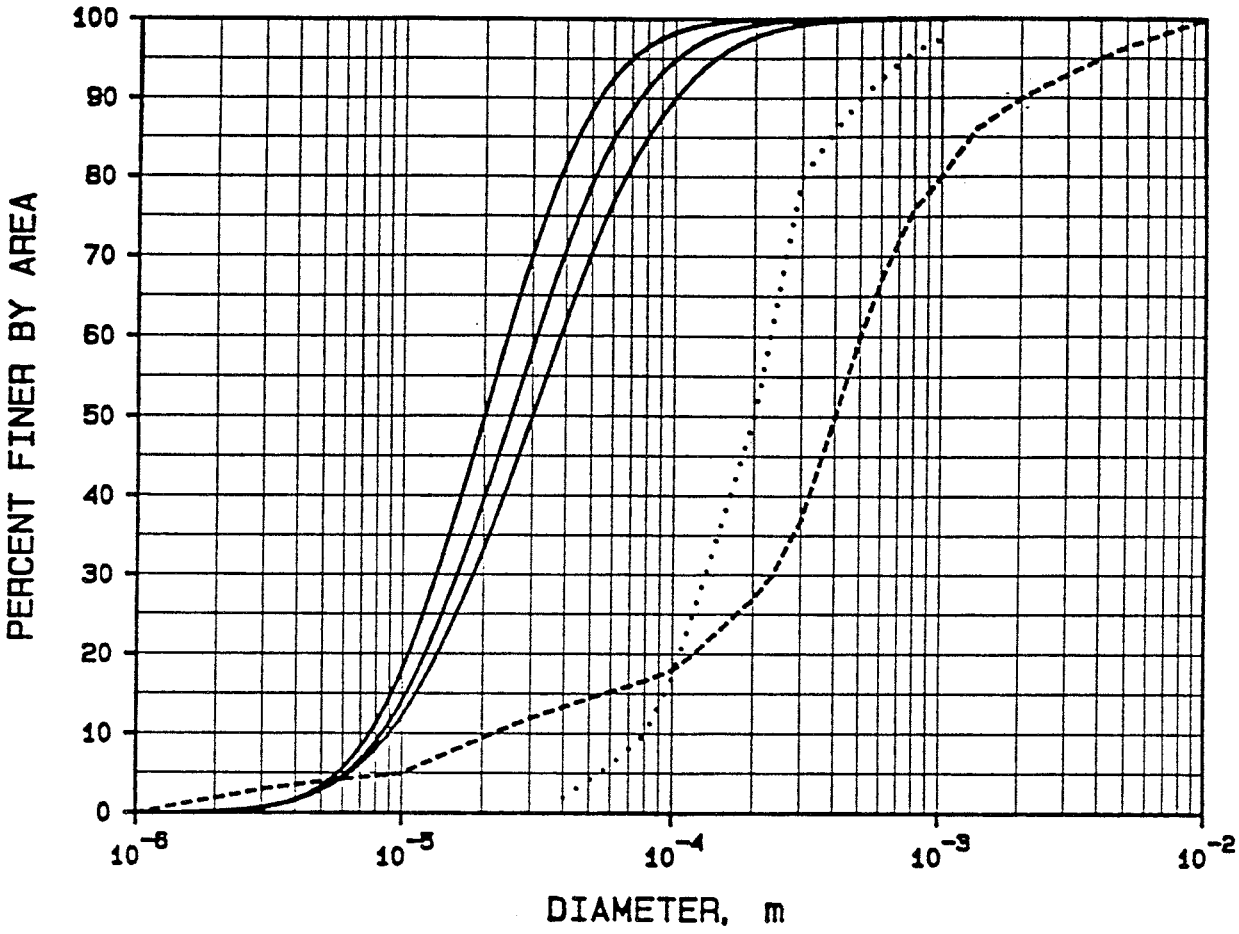

Figure 16. *Void size distributions assumed in BMT ballast mixed with 10% granulated MX-80 bentonite at 100% (solid, left), 87.5% (solid, middle) and 75% (solid, right) compaction. Also the grain size distribution of the ballast material (dashed line) and of the granulated bentonite material (dotted line) are shown in this plot.*

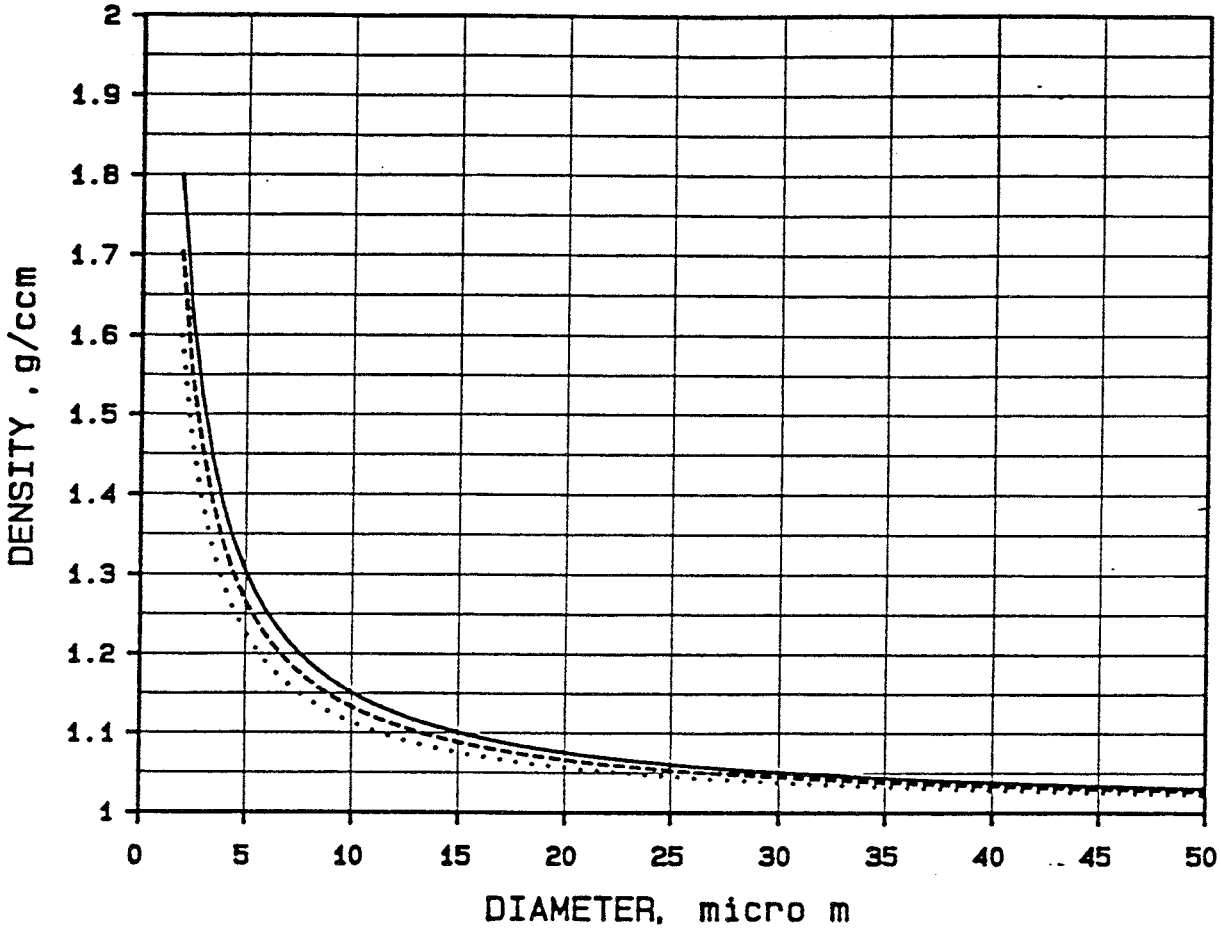

Figure 17. *Diameter-density relation used for the gel filled pores of the ballast material. The curves refer to 10% bentonite content and 100%, 87.5% and 75% compaction (dotted, dashed and solid lines, respectively).*

4.2.2 Influence of the porosity of the ballast on the physical properties of bentonitic backfills

The porosity of the ballast material (n_S) can be calculated by applying Eq. (5) while the dry density ρ_{db} of the bentonite phase, which controls both the hydraulic conductivity and the swelling pressure, is given by Eq. (6).

$$n_s = 1 - \frac{\rho_d}{\rho_s}(1-b) \tag{5}$$

where

b = bentonite content in weight percent
ρ_d = dry density of the mixture
ρ_s = specific density of the minerals

$$\rho_{db} = \rho_d - \frac{\rho_d - \rho_s(1-n_s)}{n_s} \tag{6}$$

where

ρ_{db} = dry density of the bentonite component

Hydraulic conductivity

Applying Eqs (5) and (6) and the relationships between the size of the ballast voids and the density of the clay confined in these voids one can predict the hydraulic conductivity of any mixture of ballast and bentonite. Figure 18 shows the expected conductivity of BMT materials with different bentonite contents and degrees of compaction, with Standard Proctor compaction as reference. The diagram shows that when Ca bentonite is used as clay component and this component is less than 15% and the degree of compaction is below 110%, the hydraulic conductivity will exceed 10^{-9} m/s. For 10% MX-80 in sodium form the conductivity will not exceed 10^{-10} m/s.

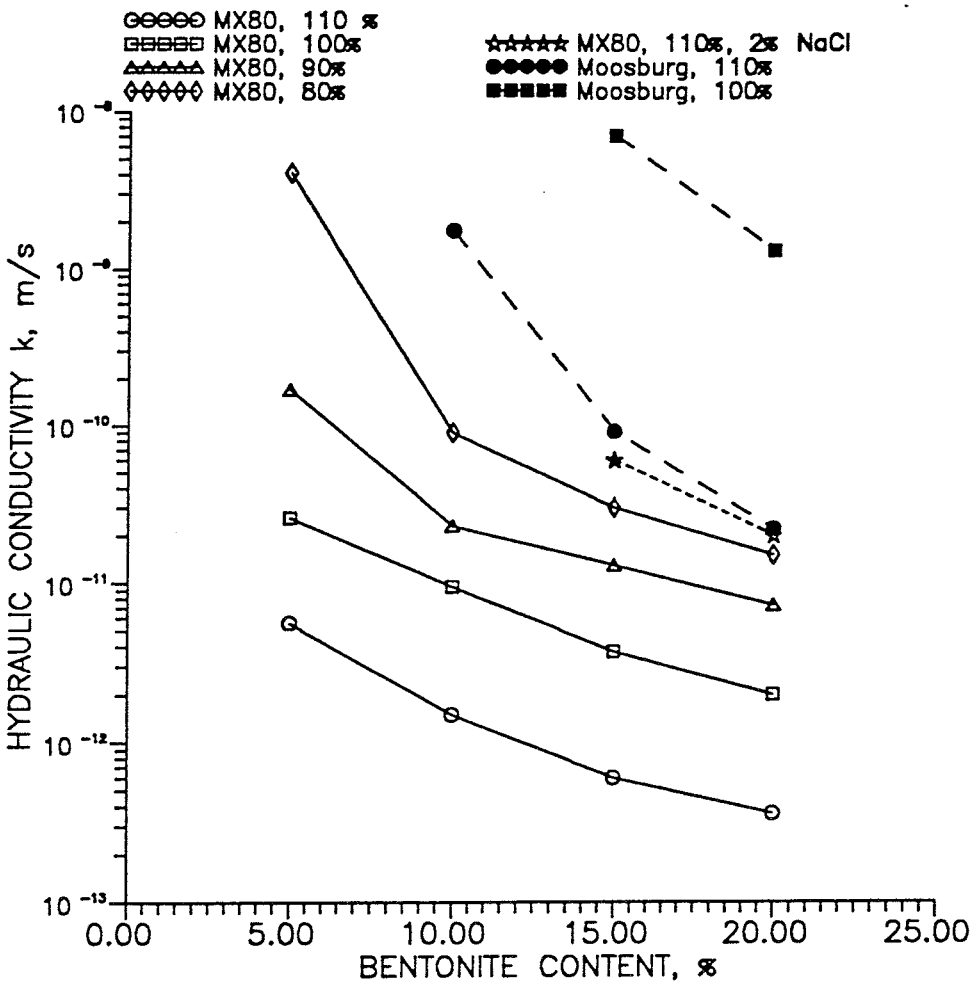

Figure 18. *Calculated hydraulic conductivities for different assumptions regarding compaction degree, bentonite type and porewater salinity. The calculations were performed assuming uniform distribution of the clay material in the voids between ballast grains. For low bentonite contents, the average density of the clay material is low, which means that in some cases, i.e. for Moosburg Ca bentonite and for saline pore water, calculations could not be based on reliable conductivity data.*
Percentages indicate degree of compaction referring to Proctor compaction..

Compressibility

The compressibility of the backfill, which, together with the hydraulic conductivity, is the major physical parameter, depends on the porosity (void ratio) as expressed by the empirical compression parameters m and β. In principle, uniaxial compression of an element Δh with thickness h is expressed as [12]:

$$\Delta h = \frac{h}{m\beta}\left[\left(\frac{\sigma'}{\sigma' j}\right)^{\beta} - \left(\frac{\sigma_0{}'}{\sigma_j{}'}\right)^{\beta}\right] \qquad (7)$$

where

m, β = strain parameters
σ' = pressure increment
σ_0' = effective pressure prior to compression
σ_j' = reference stress (100 kPa)

m ranges from 1-50 for soft soils to 100-1 000 for sand and moraine. β is commonly in the interval 0-0.7 for clays and silt soils and up to and even higher than 1.0 for rock material.

4.2.3 Stability of backfills

Piping and erosion

Piping and erosion may be of importance for the homogeneity of bentonitic backfills since high hydraulic gradients that prevail in the peripheral parts of the backfill at and shortly after the application in the tunnels may cause dispersion and washing out of fine particles, particularly smectite aggregates if the flow rate of water exceeds a critical value.

Considering first ballasts, ordinary filter criteria imply that migration of smaller grains into the voids between larger ones is largely eliminated if the network of larger grains does not contain voids that let smaller ones through. This requires Fuller- or moraine-type size distributions with no discontinuities of the part of the curves that represent D<0.1 mm. This is fairly well fulfilled by the specially composed ballast of the bottom bed of the Forsmark silo and the BMT backfill as well as all of the crushed rock materials described in the preceding text.

For bentonite/ballast mixtures the situation is different because the coherent system of stacks of flakes of smectite, i.e. the clay gel in the voids between ballast grains, can be disrupted and release a large number of small stacks under high hydraulic gradients (Figure 13). They can be transported in the direction of percolating water from the rock in conjunction with the saturation of the backfill. This process is most critical because the hydraulic gradient will initially be very high.

Experimental investigations using microscopy and special equipment for determination of the resistance to piping and erosion tests have demonstrated that there is a critical gradient for "hydraulic fracturing" of soft clay gels, like those formed in the voids between ballast grains [13].

These investigations showed that the critical gradient is on the order of 100 for clay with a density of 1.3 g/cm^3 at complete saturation. For lower densities it is down to 50 while for densities in the interval 1.3-1.45 g/cm^3, piping is not initiated until the gradient exceeds 100 [13, 14]. For higher densities, piping is not expected unless the pressure approaches the swelling pressure.

The issue is hence to investigate whether different ballast materials give different clay gel densities.

Chemical stability

Chemical degradation of smectite takes place in the form of conversion to non-expandable 10Å minerals. At the low density of the clay gel in bentonite-poor backfills such conversion implies a significant change in average hydraulic conductivity of the gel, but the residual clay still serves to give the backfill a lower hydraulic gradient than if it did not contain bentonite. The mechanism that causes conversion to non-expandable minerals is complex and can take place via formation of mixed-layer minerals or - more probably - through neoformation of illite (hydrous mica), for which Pytte's theory is assumed to be valid [15, 16]. Figure 19 shows diagrams for the conversion of smectite-to-illite according to Pytte's theory for two potassium concentrations, one being extremely high (upper diagram), and the other representing 40 ppm K^+, i.e. what is occasionally recorded at 500 m depth in crystalline rock. Both diagrams imply that the initial smectite content is unity (100%) and that the activation energy for the conversion is 27 Kcal/mole.

A second phenomenon, which is related to the illitization, is precipitation of silicious compounds and sulphates as well as carbonates. Such precipitates serve as cementing agents and may be of practical importance in the buffer material where the temperature is up to 80-90°C and the temperature gradient substantial. At temperatures lower than about 50°C and where temperature gradients do not prevail the process or occurrence of cementation is estimated to be small.

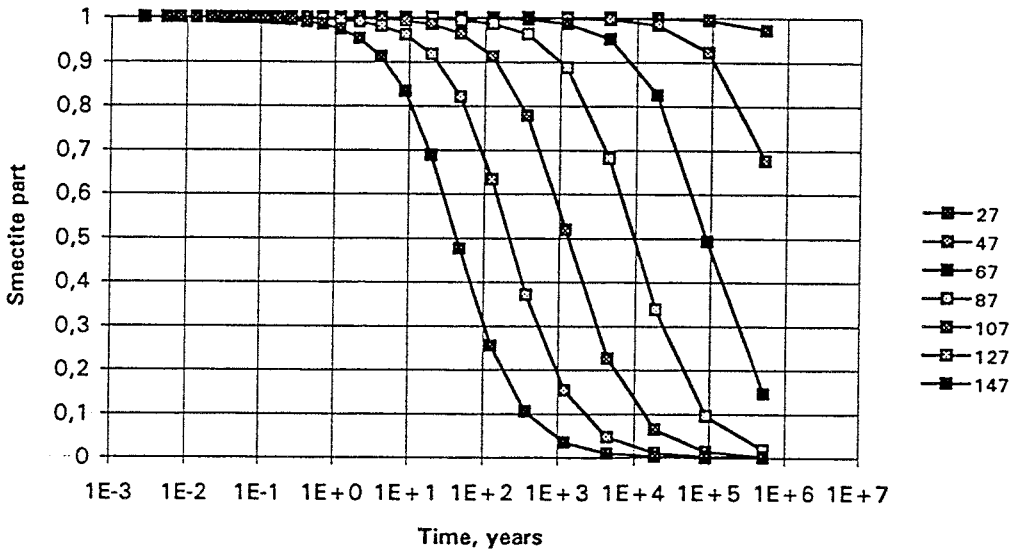

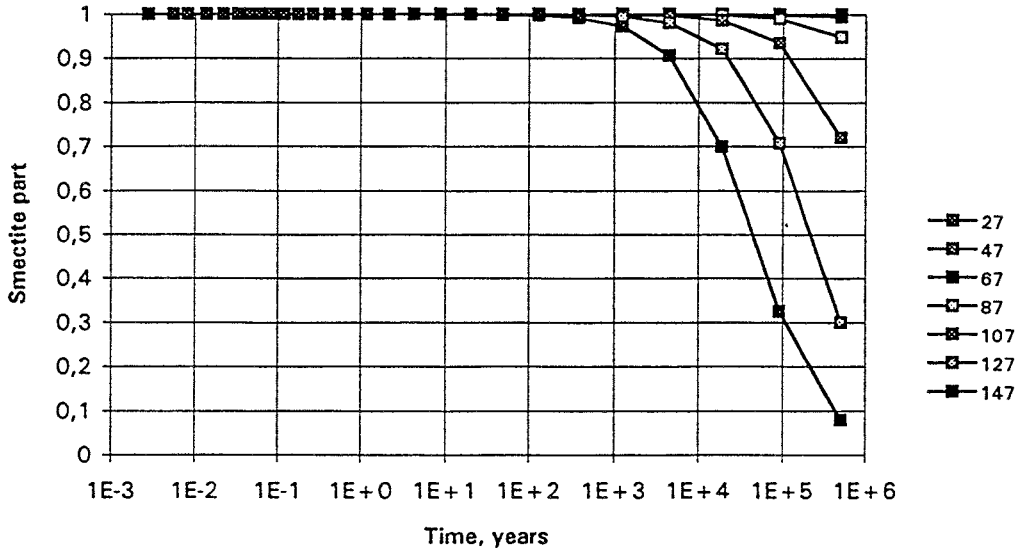

Figure 19. *Smectite-to-illite conversion rates using Pytte's theory. Upper: K^+-concentration 1 mole/l. Lower: K^+-concentration 0.001 mole/l. The curves represent different temperatures expressed in °C.*

5 BASIS OF COMPARISON OF BACKFILLS WITH QUARTZ SAND AND CRUSHED ROCK AS BALLAST COMPONENT

5.1 DEFINITION OF CANDIDATE MATERIALS

We will take here, as representatives of KBS-3 backfills with quartz sand, the Forsmark and BMT materials, and as representatives of backfills with crushed rock as ballast material, mixtures of bentonite and granitic materials from Romeleåsen and Simpevarp. As demonstrated in Chapter 4, a suitable gradation of crushed ballast very similar to that of "ideally" artificially composed ballast of glacial origin can be obtained from all sorts of crystalline rock. The selected backfills with crushed ballast are taken as typical representatives of such materials. In subsequent chapters we will compare the most important physical properties and the longevity of both types of backfills.

5.2 PHYSICAL PROPERTIES OF BACKFILLS TO BE COMPARED

5.2.1 Definitions

The hydraulic conductivity, compressibility and expandability are the major physical properties of the backfills, the compressibility being important for the displacement that results from the swelling pressure exerted by the buffer in the deposition holes, and the expandability for the ability of the backfill to maintain contact with the tunnel roof. Since the basic concept implies low-electrolyte porewater, only this type of groundwater conditions will be considered.

Backfills consisting of sand/bentonite mixtures are termed SB hereafter, while those composed of crushed rock and bentonite will be termed RB.

5.2.2 Hydraulic conductivity

SB backfills

A large number of laboratory tests of SB backfills, primarily of the type used for the silo bed at Forsmark and the BMT backfills, which had the grain size distributions shown in Figure 20, have demonstrated that the hydraulic conductivity is accurately predicted by the material model. Thus, tests with MX-80 clay and Sardinian GEKO QI bentonite with similar grain size

distribution have yielded conductivity values lower than 10^{-9} m/s also for relatively low densities as demonstrated by Table 3. The table also gives data for SB backfills ("Silver sand") with practically the same ballast gradation as the RB backfills (Figure 21).

Table 3. Hydraulic conductivity of saturated backfill materials percolated by distilled or weakly brackish water ("Allard solution")

Backfill type	Bentonite content %	Dry density g/cm^3	K m/s	Remark
SB (Forsmark)	10	1.91	4×10^{-10}	(also brackish water)
SB (Silver sand)	10	1.90	10^{-11}	
SB (Forsmark)	10	1.75	10^{-9}	
SB (BMT)	10	1.75	$\leq 10^{-9}$	
SB (Silver sand)	20	2.01	4×10^{-11}	
SB (Silver sand)	20	1.77	2×10^{-12}	100% Proctor
SB (BMT)	20	1.75	$\leq 10^{-10}$	
SB (BMT)	20	1.59	2×10^{-10}	
RB (Romeleåsen)	10	2.18	2×10^{-11}	100% Proctor
RB (Romeleåsen)[1)]	10	2.1[2)]	6×10^{-11}	100% Proctor
RB (Romeleåsen)	10	2.01	10^{-11}	"
RB (Romeleåsen)	10	1.97	9×10^{-10}	"
RB (Romeleåsen)	10	1.87	10^{-8}	10% Proctor
RB (Romeleåsen)[1)]	20	2.0[2)]	5×10^{-11}	"
RB (Romeleåsen)	20	1.88	10^{-11}	100% Proctor
RB (Romeleåsen)	20	1.79	7×10^{-12}	"
RB (Romeleåsen)	20	1.76	10^{-11}	10% Proctor

[1)] Data from [10] [2)] Estimated

RB backfills

Tests with RB backfills have been made with material with the ballast gradation shown in Figure 21. Compaction curves giving dry density values for various water contents are shown in Figure 22. The tests demonstrate that 100% Proctor compaction gives about the same densities at low water contents than at higher ones. Tests in which rounded Silver sand with almost exactly the same granular composition as the Romeleåsen material was used gave higher densities than the crushed rock. Table 3 shows that the conductivity of crushed rock with 10% bentonite and dry densities lower than 1.9-2.0 g/cm^3 is significantly higher than that of SB backfills, while the difference is less obvious for higher densities.

An important conclusion is that even very low compaction energies gave a dry density of at least 1.75 g/cm^3 of the 20% bentonite backfills mixed with crushed rock. They yielded conductivity values that were in close agreement with the ones obtained for SB materials as demonstrated by the data in Table 3.

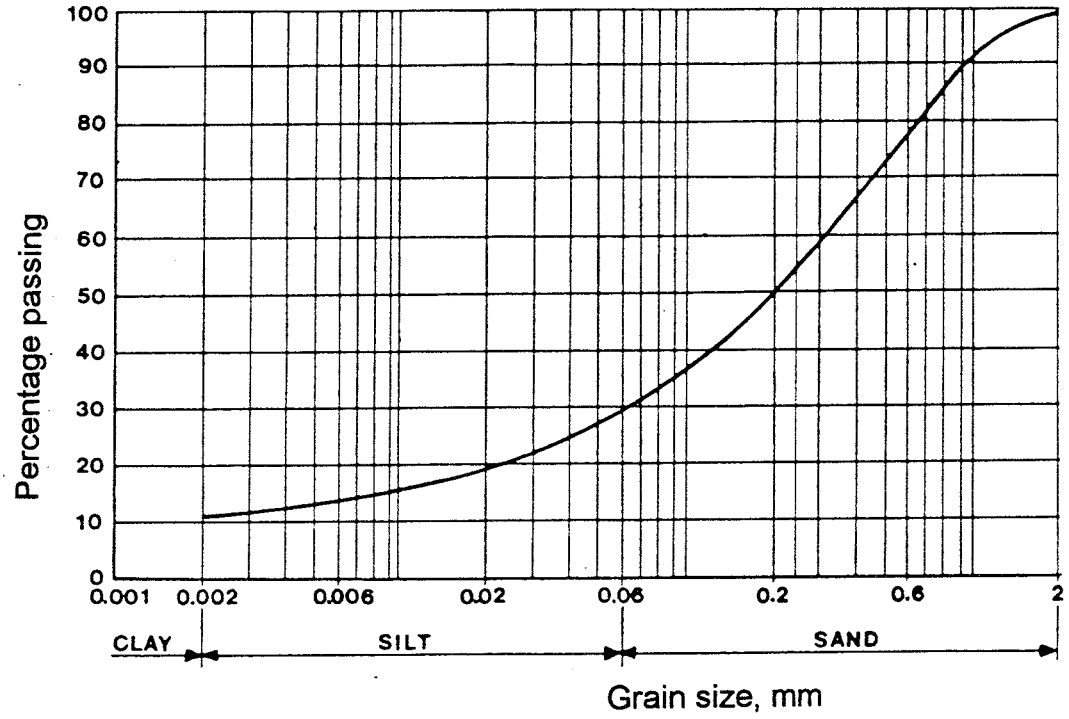

a) 10% bentonite mixture.

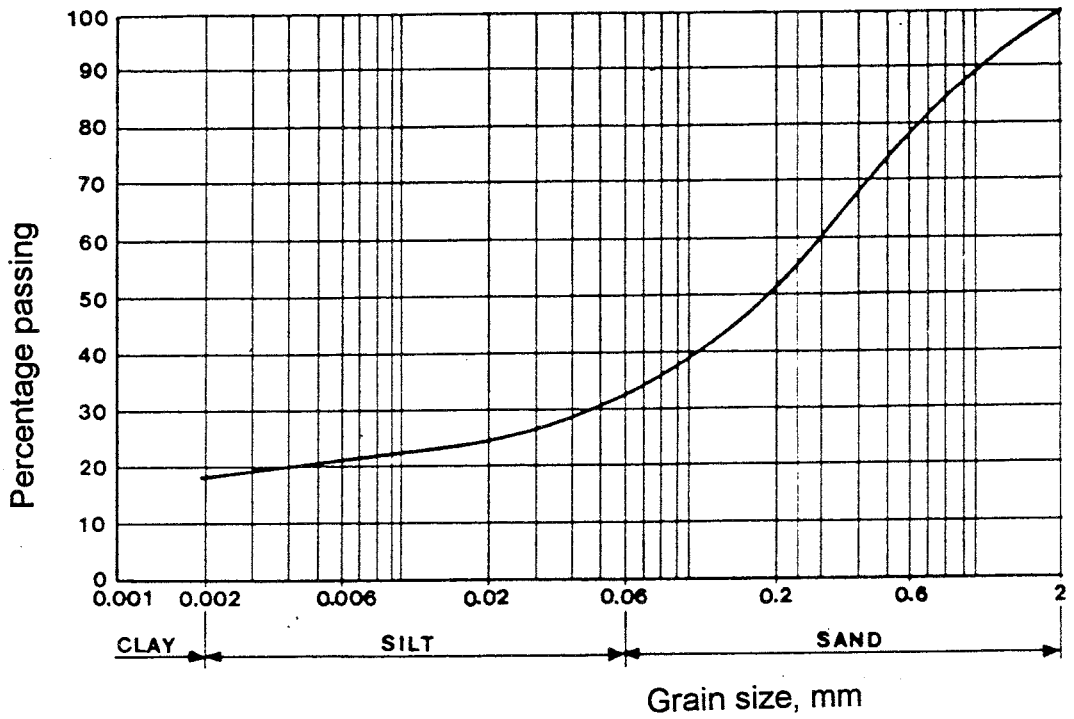

b) 20% bentonite mixture.

Figure 20. *Experimentally determined grain size distribution of 10/90 and 20/80 backfills in BMT.*

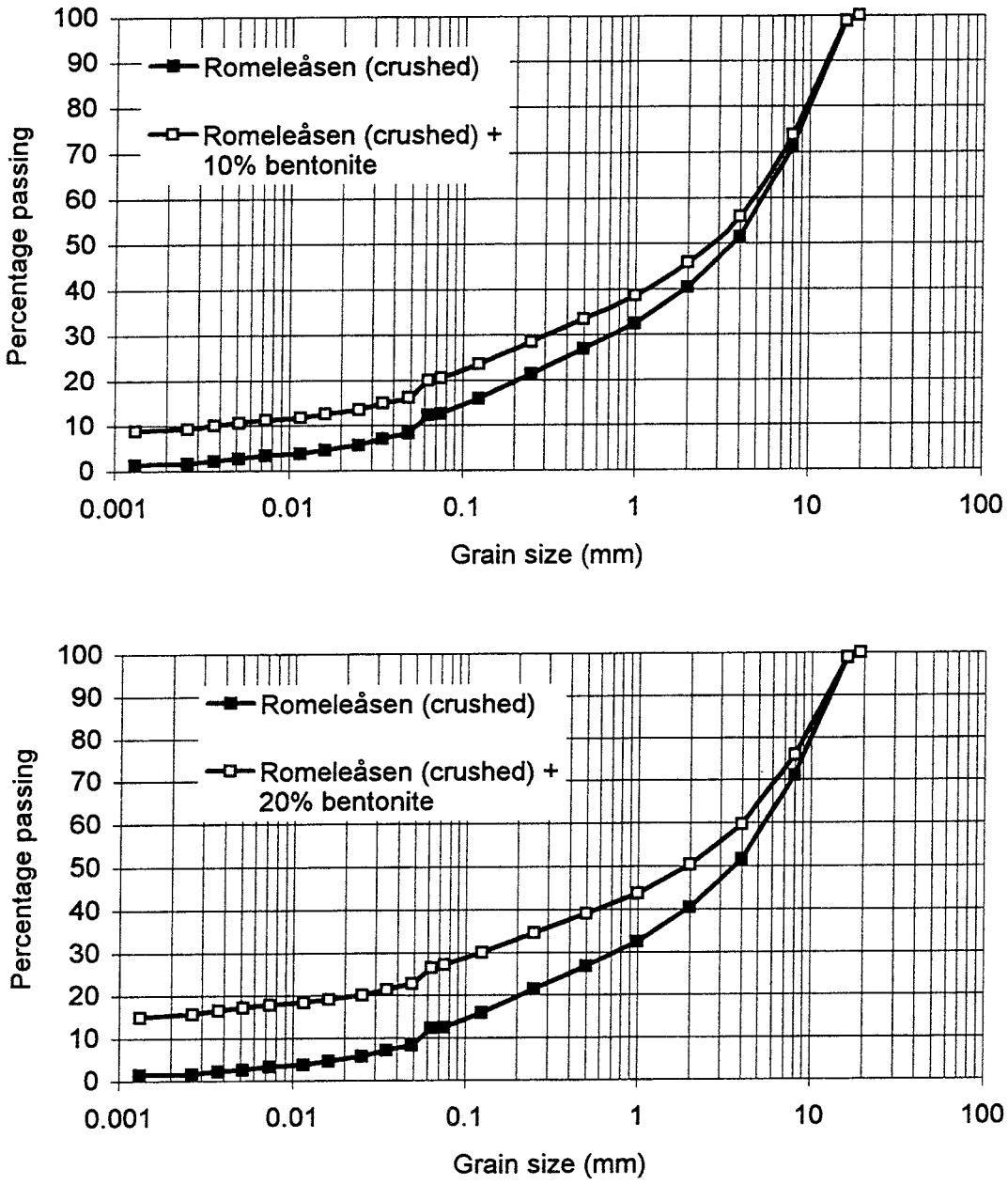

Figure 21. *Grain size distributions of 10/90 and 20/80 mixtures of crushed Romeleåsen material (cf. Figure 9) and MX-80 bentonite.*

An observation of great practical importance is that the dry density is very sensitive to the water content. Thus, even very small changes in water contents from that of optimum density (about 10%) may yield a significant drop in dry density. This is in contrast to "dry" compaction, i.e. at a water content below about 4%, which speaks in favor of dry mixing and compaction of backfills.

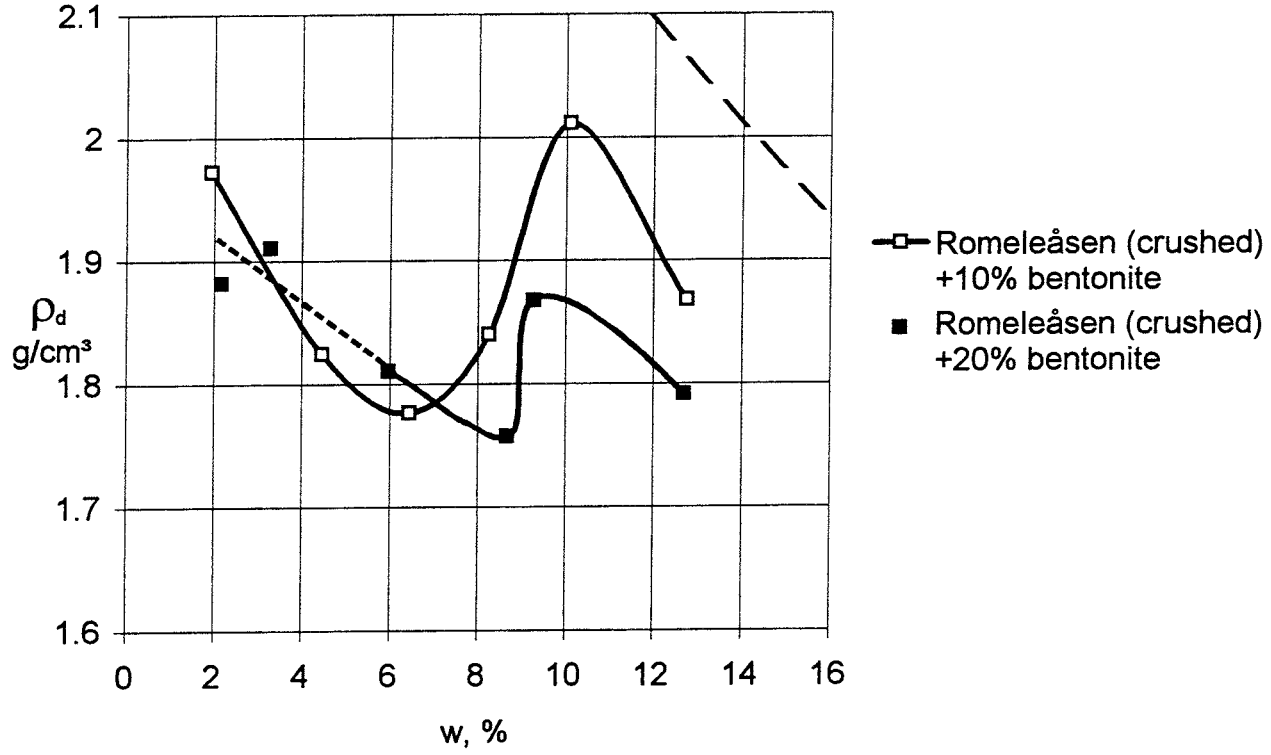

Figure 22. *"Compaction" curves (100% Proctor) for mixtures of MX-80 and crushed Romeleåsen ballast. The broken upper curve represents the theoretical maximum density with no voids in the mass.*

Conclusions

The main conclusion from the hydraulic testing is that the difference in conductivity between equally dense SB and RB backfills is negligible both for 10% and 20% bentonite contents at dry densities exceeding about 2.0 g/cm^3 and 1.8 g/cm^3, respectively.

5.2.3 Compressibility

SB backfills

The compressibility of unsaturated SB backfills has been evaluated from plate loading tests on 10/90 material used for the bottom bed of the Forsmark silo both in the laboratory and on site [17]. For the dry density of 2.15 g/cm^3 that was actually achieved, the stress exponent β was found to be 0.75 and the modulus number m = 200 MPa. Oedometer tests have been made on samples of BMT material and they have yielded the data in Table 4 [18]. There are various indications that the relative compressibility of unsaturated and saturated backfills is not very different with the exception of the rate of compression, but this needs confirmation.

Table 4. Compressibility of unsaturated backfill materials

Backfill type	Bentonite content, %	Dry density g/cm^3	Water content, %	m MPa	β
SB (Forsmark)	10	2.15	4	200	0.75
SB (BMT)	10	1.91	10	199	0.67
SB (BMT)	10	1.79	10	167	0.73
SB (BMT)	10	1.65	10	105	0.73
RB (Simp.)	15	1.90	13-15	160	0.74
RB (Simp.)	15	1.60	14.5	60	-
RB (Simp.)	15	1.30	14.8	20	0.73

RB backfills

RB backfills have been investigated using Rowe oedometers, which have a diameter of 25 cm and a height of 10 cm, thus allowing for much larger samples than ordinary 5 cm diameter oedometers do [7]. The ballast in this study was the Simpevarp material in Figure 9, mixed with 15% MX-80 bentonite to yield the complete grain size curve in Figure 23.

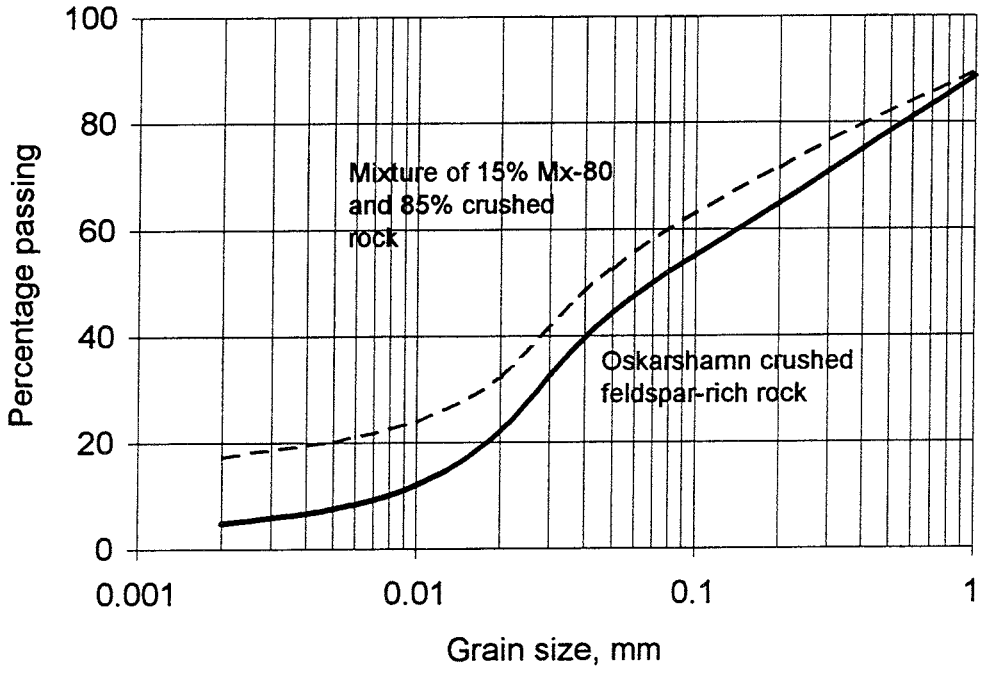

Figure 23. Grain size distribution of the Simpevarp material mixed with 15% MX-80

Conclusions

The compressibility of SB materials with 10% bentonite appears to be somewhat lower than that of the investigated RB fill with 15% bentonite. For effectively compacted fills and equal bentonite contents the opposite conditions are assumed to prevail.

Applying the Simpevarp data and assuming that the buffer in the deposition holes exerts a pressure on the backfill of 10 MPa the compression of the backfill has been estimated at 45 cm for a KBS3 tunnel [7].

5.2.4 Expandability

General

The expandability of backfills, which is of importance for their ability to maintain contact with the tunnel roof, can be expressed in terms of the swelling pressure and the expansion on reduction of the confining pressure.

SB backfills

Swelling pressure data have been reported in various contexts and relevant data are collected in Table 5. The expandability of very well compacted 10% bentonite mixtures has been found to be about 3% for a dry density of 2.15 g/cm^3, while for lower dry densities than 1.9 g/cm^3, the expansion power is negligible for this low bentonite content. For mixtures with 20% content the swelling is expected to be at least twice as high as that of the 10% mixture for the same dry density. Even at much lower densities, mixtures with 20% bentonite have an appreciable expandability, which explains why the 20/80 top backfill filled up the BMT tunnel and maintained contact with the tunnel roof despite the fact that the average dry density was not higher than about 0.8 g/cm^3 [3].

Table 5. Swelling pressure p_s of saturated backfill materials

Backfill type	Bentonite content %	Dry density g/cm^3	p_s kPa
SB (BMT)	10	2.15	400
SB (BMT)	10	2.10	170
SB (BMT)	10	1.75	150
SB (Forsmark)	10	1.75	50-100
SB (BMT)	10	1.42	20
SB (BMT)	20	1.58	200
SB (BMT)	20	1.42	100
SB (BMT)	20	1.27	50
RB (Romeleåsen)	10	2.18	575
RB (Romeleåsen)	20	1.59	70

RB backfills

Only two tests have been performed on mixtures of crushed rock and bentonite and they are reported in Table 5 as well. The data are too sparse to give a clear picture of the swelling pressure of the RB fills but there are different reasons to assume that the swelling potential of backfills with crushed rock as ballast is somewhat less than that of SB backfills. It may be explained by a somewhat higher internal friction in the firstmentioned.

Conclusions

The expandability of SB and RB backfills with a bentonite content of 10%-20% expressed in terms of swelling pressure is estimated to be of similar magnitude at least for high densities.

5.3 STABILITY

Piping and erosion

Piping and erosion tests have been performed only on SB materials but the data can be used for estimating whether the risk of flow-related degradation of the material is higher or lower for RB materials. This is made by comparing the dry density of the clay in the voids between ballast grains, for which experimental data have been published recently [19]. The study referred to in Figure 24 demonstrates that irrespective of the bentonite content, equally compacted SB and RB materials had practically identical clay densities.

BMT-type backfills have been tested in order to simulate the conditions when a freshly applied backfill with 18% bentonite is exposed momentarily to a water pressure of 100 kPa [20]. The mixture had a dry density of 1.41 g/cm^3 and an initial water content of 18%. When the test was terminated after 9 days, the distribution of the clay content was found to be unaltered.

It is expected that RB backfills are somewhat more sensitive to piping and erosion than SB backfills despite the similar average clay density in the ballast voids. This is because the splintery factor is higher for crushed rock than for rounded glacial material, which yields more narrow voids at the junction points of adjacent ballast grains. Even for well rounded ballast material the most narrow voids will not be filled with clay as illustrated by Figure 25 [21]. RB backfills hence represent a somewhat higher risk of piping and erosion.

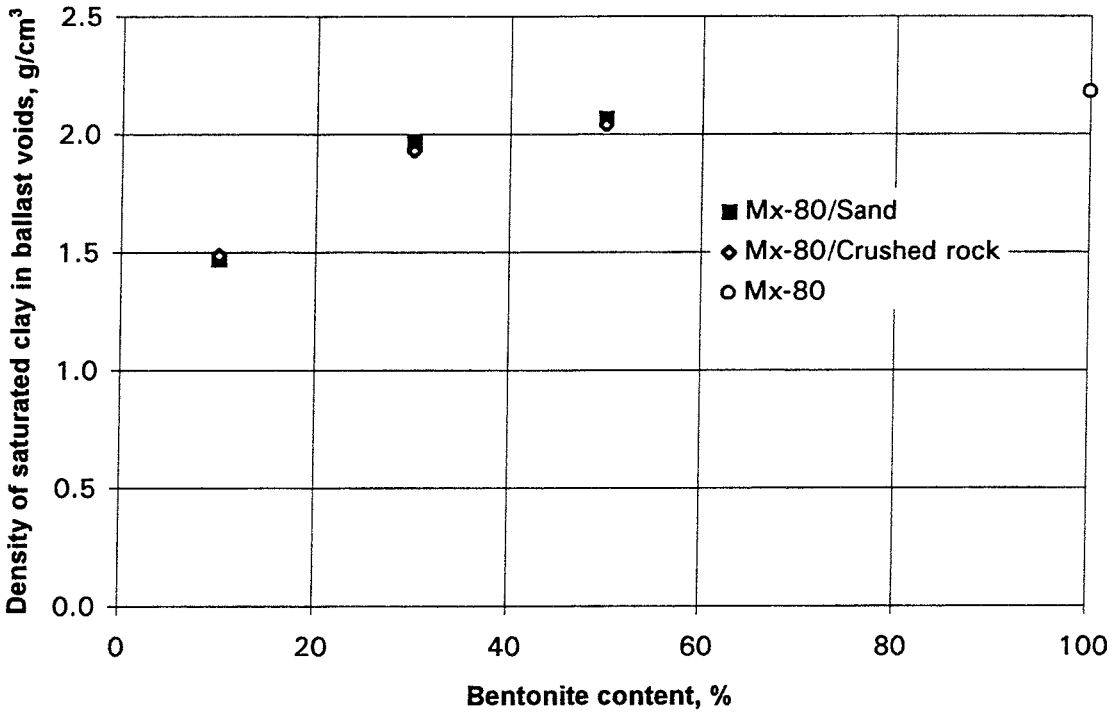

Figure 24. *Density of the saturated clay contained in the voids of SB (Silver sand) and RB (Romeleåsen) fills, compacted to 100% Proctor energy.*

Conclusions

The difference in average density of the clay contained in the ballast voids in SB and RB backfills is negligible at least for effective compaction. However, the expected stronger heterogeneity of the RB clay implies that the risk of piping and erosion is somewhat higher for this sort of backfill.

Chemical stability

The matter of chemical stability is related to the solubility and release of potassium as outlined earlier in the report. For SB material with ballast consisting of quartz grains the ballast will not provide any potassium at all for smectite→illite conversion. For RB fills the conditions are as follows.

Using the average diameter ratios b/a=0.5 and c/b=0.3 (cf. Figure 5), ordinary crushed rock material with grain size distributions of the types discussed in Chapter 4 yield a surface area of the type shown in Table 6.

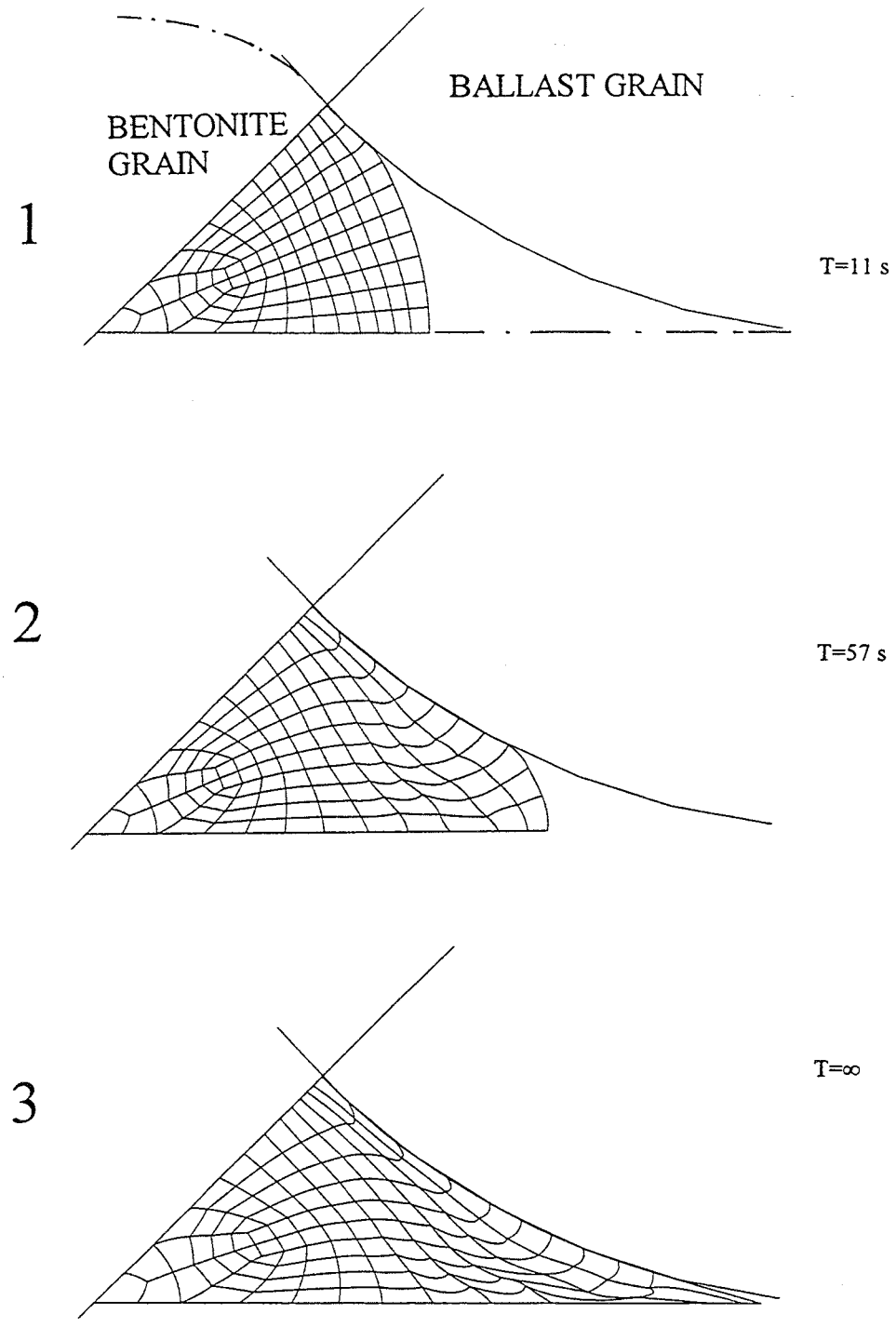

Figure 25. *Expansion of 0.5 mm bentonite "grain" with an initial dry density of 2.29 g/cm^3 in the ballast voids [21]. The outermost part of the gel in the final expansion stage has a dry density of 0.65 g/cm^3 (ρ_{sat}=1.42 g/cm^3), while the densest left part has a dry density of about 1.45 g/cm^3 (ρ_{sat}=1.93 g/cm^3)*

Table 6. Approximate surface area of different size fractions for the standard ("100%") case. ρ_d = 1.5 t/m^3

Size fraction mm	Number of grains per m^3	Surface area m^2 per m^3
0.006 - 0.06	10^{14}	$5 \cdot 10^4$
0.06 - 0.6	10^{11}	$5 \cdot 10^3$
0.6 - 6	10^8	$5 \cdot 10^2$
> 6	$5 \cdot 10^5$	250

Granite commonly contains 10-30% (weight %) quartz, 10-50% feldspars, 10-20% heavy minerals and 1-5% mica. The dominant rock type at Äspö, the Äspö diorite, holds some 15-25% K-feldspars (orthoclase + microcline) and 5-10% biotite, while the fine-grained granite holds about 40% K-feldspar and a few percent biotite. The so-called Ävrö granite holds 25-35% K-feldspars and about 5% biotite.

Using the figure for the surface area of the ballast of Äspö TBM type in Table 6, i.e. about $5 \cdot 10^4$ m^2/m^3, and taking the K-feldspar content as 30% one finds that the amount of released potassium is not a constraint of the conversion, i.e. the amount of dissolved potassium is sufficient to yield complete conversion from smectite to illite. However, in practice such conversion will be negligible as demonstrated by the diagrams in Figure 19. Thus, the temperature in the lower part will not exceed about 40°C, which means that even at the high K^+ concentration, only a few percent of the smectite content will be converted to illite in the few thousand years during which the temperature exceeds 10-15°C [22].

The rather low temperature and significantly lower temperature gradient in the backfill than in the canister-embedding buffer mean that significant cementation effects are not expected, but substantial evidence for this standpoint is not at hand.

The change in physical performance by ion exchange phenomena like Na to Ca in backfills with a low content of bentonite but suitable ballast granulometry is known to be of very moderate influence, especially at high densities [5]. However, for unsuitably graded ballast with low densities, the influence of changes in porewater chemistry may be significant.

6 DISCUSSION

6.1 COMPARISON OF PHYSICAL PROPERTIES OF SB AND RB BACKFILLS

A major conclusion is that ballast material obtained by crushing crystalline rock normally gets a gradation that is of Fuller's type and, depending on the crushing procedure, with a suitably low D_5. Hence, in this respect the ballast has a form that is equally good as that of artificially composed granular material of glacial origin. However, the angular shape of the crushed rock particles and their rough surfaces give somewhat lower densities at compaction than do glacial materials.

The dry density of Proctor compacted air-dry mixtures of SB backfills with 10% bentonite is estimated to be 5% higher than that of RB mixtures and this appears to be the case also for 20% bentonite. These differences mean that all important physical properties, except the compressibility, are somewhat less good for RB mixtures, which can be compensated either by more effective compaction or by increasing the bentonite content somewhat.

The compactability is hence a major issue that needs consideration. A laboratory-scaled study that is of some value in the present context is illustrated in Figure 26, which shows the compression under static pressure of crushed granite with a grain size distribution similar to that of curve 7 in Figure 8, compacted by applying different energies [23]. The reference compaction procedure was a Proctor-like process using a 4.5 kg weight falling freely from 50 cm height, corresponding to a compaction energy of 2.5×10^3 kNm/m^3, while the other compaction efforts were made by changing the mass and fall height of the weight so as to yield 450% (λ=4.5), 57% (λ=0.57), 12% (λ=0.12) and 4% (λ=0.04) of the reference compaction energy (λ=1).

The plate loading tests revealed that compaction up to λ=0.57 and subsequent plate loading up to 2 MPa bring the virtually intact particles in effective contact, while lower energies lead to substantial displacements and breakage of the particles also at moderate plate loads. An interesting fact is that heavy compaction effectively reduced the compressibility. Experience tells that field compaction applying ordinary vibration rollers often yield more than 100% Proctor density. Special efforts, like increasing the number of passages from about 10 to 20 in the compaction of the 10/90 backfill in the lower part of the tunnel, is expected to yield 110% Proctor density. This would be sufficient to give RB backfills hydraulic and swelling properties that are equally good as those of SB backfills compacted to 100% Proctor density.

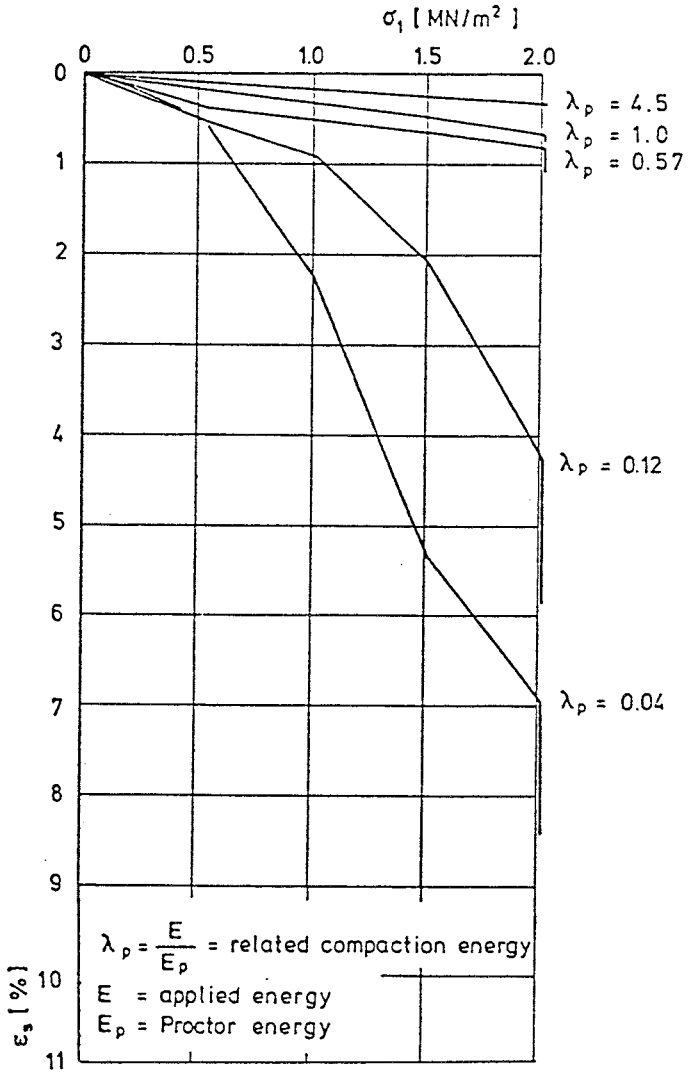

Figure 26. Compression tests of differently compacted crushed granite rockfill [23]

6.2 ESTIMATED DENSITY OF THE BACKFILL

6.2.1 Modes of application and compaction of the backfill

The procedure assumed in the basic concept for applying the 10/90 backfill in the lower part of the tunnels, i.e. layerwise application of air-dry material and compaction by vibratory rollers, can be applied for both SB and RB backfills. The assumed dry density for SB backfills 1.75-2.15 g/cm^3 (cf. Chapter 2.1), can be achieved also for RB backfills and it is expected that an increased number of roller passages will in fact yield a minimum value of ρ_d=2.0 g/cm^3.

For the upper part of the tunnels, which will be filled by shotcreting 20/80 SB backfill according to the basic concept, the expected dry density will be in the range of 1.0-1.6 g/cm^3 (cf. Chapter 2.1). This technique may be

applicable also to RB backfills although the presence of larger grains, which are suitable for optimum gradation, may present practical problems. Since improved techniques are desired for getting a more homogeneous mass of higher density, alternative methods are being investigated. One has the form of lateral application by use of special tractors to form steep layers which are compacted by use of a vibrator attached to the blade, as illustrated by Figure 27.

This technique is expected to yield a higher density than shotcreting, a probable minimum value being ρ_d=1.25-1.5 g/cm^3. Still, a conservative and safe assumption would be the density distribution indicated in the figure, i.e. ρ_d=1.0 g/cm^3 at the roof contact and ρ_d=1.5 g/cm^3 at 1 m depth below the roof. The rest of the top backfill is expected to be compacted to a dry density that increases linearly to 2.0 g/cm^3 at the upper boundary of the lower 10/90 backfill.

With these assumptions the major physical properties of SB material applied according to the basic concept, and those of RB material applied in the alternative fashions with more effective compaction of the 10/90 part and with lateral compaction would yield the estimated data in Table 7. We see from this table that the specified physical properties are similar for the two types of backfill and it can be assumed that also the compressibility and piping and erosion resistance are similar.

Table 7. Comparison of major physical data of SB backfill according to the basic concept and RB backfill applied in alternative fashions

Backfill	Bentonite/ballast ratio	Dry density g/cm^3	Hydr. cond. m/s	Swelling pres. kPa
SB bottom part	1:10	1.75 - 2.15	10^{-11} - 10^{-9}	150-400
RB bottom part	1:10	2.0 - 2.15	$5x10^{-11}$ - $8x10^{-10}$	100-200
SB top part	1:5	1.0 - 1.64	$5x10^{-10}$ - $5x10^{-11}$	0-200
RB top part	1:5	1.0 - 2.0	10^{-9} - $5x10^{-11}$	0-300

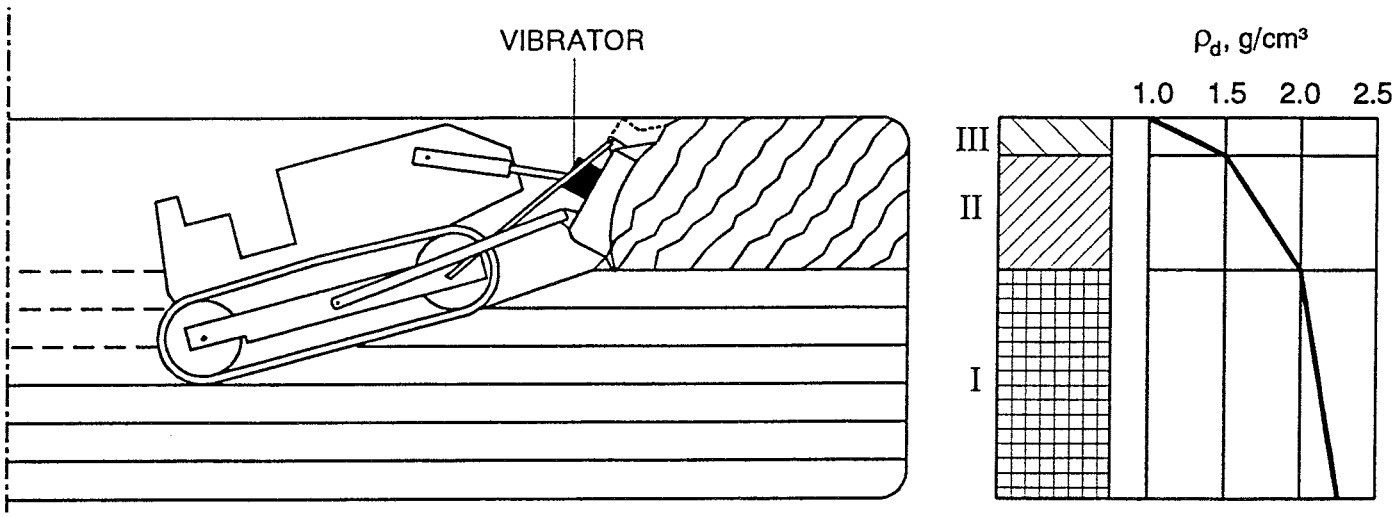

Figure 27. Assumed dry density distribution in RB backfill

7 CONCLUSIONS

The study has given the following major results:

1. Crushing of crystalline rock for ballast production can give a grain size distribution that yields the desired physical properties of RB backfills (cf. section 3).

2. Compaction of RB backfills to yield any defined dry density requires more energy than SB backfills, which, if required, probably can be achieved by increasing the number of passages of the vibratory roller over the lower 10/90 backfill and by applying lateral vibratory compaction of the upper 20/80 backfill.

3. An alternative to increase the density by more effective compaction in order to obtain a RB backfill that performs equally well as a SB backfill is to increase the bentonite content. The required increase is estimated to imply a bentonite content of 15% in the lower part of the backfill and 30-40% in the upper part.

4. It is estimated that, regardless of whether SB or RB backfills are used, a firm contact between the backfill and the roof requires an increase in bentonite content to at least 30% in order to compensate the drop in expandability that results from uptake of salt water and from cation exchange to Ca-state. This matter needs more consideration in the design work.

5. The chemical stability of backfills with quartz sand or crushed granitic rock with K-bearing minerals as ballast is estimated to be similar in the deposition tunnel backfill.

REFERENCES

1. **SKB**. PLAN 94

2. **SKB**. Anläggningsbeskrivning AR 44-93-005

3. **Pusch, R. & Nilsson, J**. Buffer Mass Test - Rock Drilling and Civil Engineering. Stripa Project, Int. Report 82-07, SKB, Stockholm, 1982

4. **Pusch, R. & Börgesson, L**. PASS - Project on Alternative Systems Study: Performance Assessment of Bentonite Clay Barrier in Three Repository Concepts: VDH, KBS-3 and VLH, SKB Technical Report TR 82-40, SKB Stockholm, 1992

5. **Pusch, R**. Waste Disposal in Rock. Developments in Geotechnical Engineering, 76. Elsevier Publ. Co., 1994

6. **Andreasson, L**. Kompressibilitet hos friktionsjord. Doctoral Thesis, Chalmers University of Technology, Gothenburg, Sweden, 1973

7. **Holopainen, P., Pirhonen, V. & Snellman, M**. Crushed aggregate-bentonite mixtures as backfill material for the Finnish repositories low- and intermediate-level radioactive wastes. Nuclear Waste Commission of Finnish Power Companies, YJT-84-07, 1984

8. **Knutsson, S. & Pusch, R.** Laboratorieundersökningar av kompressionsegenskaperna hos tunnelfyllning av bentonit/bergkross. Internal Report, University of Luleå, March 3, 1978 (Unpublished)

9. **Kenney, T.C., Lau, D. & Ofoegbu, G.I.** Permeability of compacted granular materials. Canadian Geotechnical Journal, No. 4, Vol. 21, 1984 (pp. 726-729)

10. **Pusch, R. & Hökmark, H.** Bentonite/ballast backfills. SKB Arbetsrapport AR 90-50, SKB, Stockholm

11. **Pusch, R., Karnland, O. & Hökmark, H.** GMM - A general microstructural model for qualitative and quantitative studies of smectite clays. SKB Technical Report TR 90-43, SKB Stockholm 1990

12. **Janbu, N.** Grunnlag i Geoteknikk. Tapir Forlag, Trondheim, 1970

13. **Pusch, R., Karnland, O., Hökmark, H. Sandén, T. & Börgesson, L.** Final Report of the Rock Sealing Project - Sealing Properties and Longevity of Smectitic Clay Grouts. Stripa Project Technical Report TR 91-30, SKB, Stockholm, 1991

14. **Pusch, R., Hökmark, H. & Börgesson, L.** Outline of models of water and gas flow through smectite clay buffers. SKB Technical Report TR 87-10, SKB, Stockholm, 1987

15. **Pusch, R.** Evolution of models for conversion of smectite to non-expandable minerals. SKB Technical Report TR 93-33, SKB, Stockholm, 1993

16. **Pusch, R. & Madsen, F.** Aspects of illitization of Kinnekulle bentonites. Clay and Clay Minerals (In print), 1995

17. **SKB**. Review and Study on Design and Construction of Bentonite Buffers in the SFR Repository, and Aspects of Future Storages of SFR Type in Japan. SKB, Stockholm, 1992

18. **Pusch, R. & Börgesson, L.** Buffer Mass Test - Buffer Materials. Stripa Project Internal Report 82-06, SKB, Stockholm, 1982

19. **Börgesson, L., Johannesson, L-E. & Fredrikson, A.** Laboratory investigations of highly compacted sand/bentonite blocks for backfilling. Compaction technique, material properties and repository function. SKB Project Report PR 44-93-010. SKB, Stockholm, 1993

20. **Pusch, R.** Clay particle redistribution and piping phenomena in bentonite/quartz buffer material due to high hydraulic gradients. SKB Teknisk Rapport KBS 18, SKB, Stockholm, 1979

21. **Börgesson, L.** Swelling and homogenisation of bentonite granules in buffer and backfill. SKB Arbetsrapport, Dec. 1994 (In print)

22. **Hökmark, H.** Smectite-to-illite conversion in bentonite buffers. SKB AR 95-07, SKB, Stockholm, 1994

23. **Brauns, J., Kast, K. & Blinde, A.** Compaction effects on the mechanical and saturation behavior of disintegrated rockfill. International Conf. on Compaction, Vol. I, Laboratoire Central des Ponts et Chausses, Paris 1980 (pp. 107-112)

List of SKB reports

Annual Reports

1977-78
TR 121
KBS Technical Reports 1 – 120
Summaries
Stockholm, May 1979

1979
TR 79-28
The KBS Annual Report 1979
KBS Technical Reports 79-01 – 79-27
Summaries
Stockholm, March 1980

1980
TR 80-26
The KBS Annual Report 1980
KBS Technical Reports 80-01 – 80-25
Summaries
Stockholm, March 1981

1981
TR 81-17
The KBS Annual Report 1981
KBS Technical Reports 81-01 – 81-16
Summaries
Stockholm, April 1982

1982
TR 82-28
The KBS Annual Report 1982
KBS Technical Reports 82-01 – 82-27
Summaries
Stockholm, July 1983

1983
TR 83-77
The KBS Annual Report 1983
KBS Technical Reports 83-01 – 83-76
Summaries
Stockholm, June 1984

1984
TR 85-01
Annual Research and Development Report 1984
Including Summaries of Technical Reports Issued during 1984. (Technical Reports 84-01 – 84-19)
Stockholm, June 1985

1985
TR 85-20
Annual Research and Development Report 1985
Including Summaries of Technical Reports Issued during 1985. (Technical Reports 85-01 – 85-19)
Stockholm, May 1986

1986
TR 86-31
SKB Annual Report 1986
Including Summaries of Technical Reports Issued during 1986
Stockholm, May 1987

1987
TR 87-33
SKB Annual Report 1987
Including Summaries of Technical Reports Issued during 1987
Stockholm, May 1988

1988
TR 88-32
SKB Annual Report 1988
Including Summaries of Technical Reports Issued during 1988
Stockholm, May 1989

1989
TR 89-40
SKB Annual Report 1989
Including Summaries of Technical Reports Issued during 1989
Stockholm, May 1990

1990
TR 90-46
SKB Annual Report 1990
Including Summaries of Technical Reports Issued during 1990
Stockholm, May 1991

1991
TR 91-64
SKB Annual Report 1991
Including Summaries of Technical Reports Issued during 1991
Stockholm, April 1992

1992
TR 92-46
SKB Annual Report 1992
Including Summaries of Technical Reports Issued during 1992
Stockholm, May 1993

1993
TR 93-34
SKB Annual Report 1993
Including Summaries of Technical Reports Issued during 1993
Stockholm, May 1994

1994

TR 94-33

SKB Annual Report 1994

Including Summaries of Technical Reports Issued during 1994.
Stockholm, May 1995

List of SKB Technical Reports 1995

TR 95-01

Biotite and chlorite weathering at 25°C. The dependence of pH and (bi) carbonate on weathering kinetics, dissolution stoichiometry, and solubility; and the relation to redox conditions in granitic aquifers

Maria Malmström[1], Steven Banwart[1], Lara Duro[2], Paul Wersin[3], Jordi Bruno[3]
[1] Royal Institute of Technology, Department of Inorganic Chemistry, Stockholm, Sweden
[2] Universidad Politécnica de Cataluña, Departmento de Inginería Química, Barcelona, Spain
[3] MBT Tecnología Ambiental, Cerdanyola, Spain
January 1995

TR 95-02

Copper canister with cast inner component. Amendment to project on Alternative Systems Study (PASS), SKB TR 93-04

Lars Werme, Joachim Eriksson
Swedish Nuclear Fuel and Waste Management Co, Stockholm, Sweden
March 1995

TR 95-03

Prestudy of final disposal of long-lived low and intermediate level waste

Marie Wiborgh (ed.)
Kemakta Konsult AB, Stockholm, Sweden
January 1995

TR 95-04

Spent nuclear fuel corrosion: The application of ICP-MS to direct actinide analysis

R S Forsyth[1], U-B Eklund[2]
[1] Caledon-Consult AB, Nyköping, Sweden
[2] Studsvik Nuclear AB, Nyköping, Sweden
March 1995

TR 95-06

Palaeohydrological implications in the Baltic area and its relation to the groundwater at Äspö, south-eastern Sweden – A literature study

Bill Wallin
Geokema AB, Lidingö, Sweden
March, 1995

TR 95-07

Äspö Hard Rock Laboratory Annual Report 1994

SKB
April 1995

TR 95-08

Feasibility study for siting of a deep repository within the Storuman municipality

Swedish Nuclear Fuel and Waste Management Co., Stockholm
January 1995

TR 95-09

A thermodynamic data base for Tc to calculate equilibrium solubilities at temperatures up to 300°C

Ignasi Puigdomènech[1], Jordi Bruno[2]
[1] Studsvik AB, Nyköping, Sweden
[2] Intera Information Technologies SL, Cerdanyola, Spain
April 1995

TR 95-10

Investigations of subterranean microorganisms. Their importance for performance assessment of radioactive waste disposal

Karsten Pedersen[1], Fred Karlsson[2]
[1] Göteborg University, General and Marine Microbiology, The Lundberg Institute, Göteborg, Sweden
[2] Swedish Nuclear Fuel and Waste Management Co., Stockholm, Sweden
June 1995

TR 95-11

Solute transport in fractured media – The important mechanisms for performance assessment

Luis Moreno, Björn Gylling, Ivars Neretnieks
Department of Chemical Engineering and Technology, Royal Institute of Technology, Stockholm, Sweden
June 1995

TR 95-12

Literature survey of matrix diffusion theory and of experiments and data including natural analogues

Yvonne Ohlsson, Ivars Neretnieks
Department of Chemical Engineering and Technology, Royal Institute of Technology, Stockholm, Sweden
August 1995

TR 95-13

Interactions of trace elements with fracture filling minerals from the Äspö Hard Rock Laboratory

Ove Landström[1], Eva-Lena Tullborg[2]
[1] Studsvik Eco & Safety AB
[2] Terralogica AB
June 1995